EXTERNAL BOUNDARY LAYERS IN AQUEOUS POLYMER SOLUTION FLOWS

AN EXPERIMENTAL STUDY OF THE BOUNDARY LAYER FORMED ON A FLAT PLATE IN A DILUTE HOMOGENEOUS POLYMER SOLUTION

By

J. Arthur Middleton, B.Eng.

A Thesis

Submitted to the Faculty of Graduate Studies

in Partial Fulfilment of the Requirements

for the Degree

Master of Engineering

McMaster University

June 1969

MASTER OF ENGINEERING (1969)
(Mechanical Engineering)

McMASTER UNIVERSITY
Hamilton, Ontario

TITLE: An Experimental Study of the Boundary Layer Formed on a Flat Plate in a Dilute Homogeneous Polymer Solution

AUTHOR: J. Arthur Middleton, B.Eng. (McMaster University)

SUPERVISOR: Dr. B. Latto

NUMBER OF PAGES: vii, 84

SCOPE AND CONTENTS:

This thesis describes an experimental study of external boundary layers formed on a flat plate model immersed in dilute homogeneous polymer solutions.

The model was subjected to flows of homogeneous aqueous polyacrylamide solutions with a free stream velocity of 2.21 feet per second.

Variations in the drag force with respsct to solution concentration were assessed from extensive velocity profile data and direct drag measurements. For the flow conditions a maximum reduction in total drag of 33 per cent occurred for a concentration of 50 wppm. Profile drag, as well as viscous drag, is apparently reduced in dilute polymer solutions. For the polymer used, a critical wall shear stress of 0.011 lb_f/ft^2. was found below which no reduction in viscous drag occurs.

ACKNOWLEDGEMENTS

The author wishes to thank Dr. B. Latto, under whose guidance this research was carried out, for his understanding, encouragement and assistance during the course of this program.

Thanks are also extended to Mr. T. Kowalski whose example and advice have been invaluable to the author.

The author would also like to express his gratitude to Mr. P. Zachar for his assistance in computations.

Polymer samples, supplied by Stein-Hall Limited of Westhill, Ontario, free of charge, are gratefully acknowledged.

This research was supported financially by the Defence Research Board of Canada, under grant number, 9550-25.

TABLE OF CONTENTS

Table of Contents Cont'd

NOMENCLATURE

SYMBOL	DESCRIPTION	UNITS
A	Numerical constant in the universal logarithmic velocity profile for turbulent flow.	
B	Numerical constant in the universal logarithmic velocity profile for turbulent flow.	
C_f	Local coefficient of skin friction $= \left(\frac{\tau_o}{(\rho U_1^2/2)}\right)$	
D	Drag force	lb_f
k	Prandtl's mixing length constant	
L	Length of flat plate model	ft
N	Exponent in shear stress correlation	
Re_x	Reynolds number $= \left(\frac{xU_1}{\nu}\right)$	
u	Average velocity in direction of mean flow at a point	ft/sec.
U_1	Average velocity at edge of boundary layer at a plane in the direction of flow	ft/sec.
U_∞	Free stream velocity	ft/sec.
U^*	Friction velocity $= (\tau_o/\rho)^{1/2}$	
U^*_c	Critical friction velocity $= (\tau_{o_c}/\rho)^{1/2}$	ft/sec.
U^+	Non-dimensional velocity $= (u/U^*)$	
x	Distance along plate from leading edge	ft.
w_c	Critical wave number U^*_c/ν	1/ft.

SYMBOL	DESCRIPTION	UNITS
y	Distance normal to plate surface	ft.
Y^+	Non-dimensional distance = $(\frac{yU^*}{\nu})$	ft.
θ	Momentum thickness $\int_0^\infty (1 - \frac{u}{U_1}) \frac{u}{U_1} dy$	ft.
ν	Kinematic viscosity of fluid	$ft^2/sec.$
τ_o	Wall shear stress $\mu(\frac{\partial u}{\partial y})_{y=0}$	lb_f/ft^2
τ_{o_s}	Wall shear stress of solvent at some boundary layer thickness	lb_f/ft^2
τ_{o_p}	Wall shear stress of polymer solution at some boundary layer	lb_f/ft^2
τ_{o_c}	Critical wall shear stress	lb_f/ft^2
ρ	Density of fluid	lb_m/ft^3

Abbreviations

wppm — weight parts per million weight parts of water

CHAPTER I

INTRODUCTION:

The effect on viscous drag due to the presence of certain additives in aqueous solutions has been known for some time. Most of the information presently available is concerned with internal flows, such as pipe flow. This path has been followed mainly for reasons of convenience. However, recently more emphasis has been placed on the effects of additives, for example long-chain polymers on external flows, such as that of liquids over a flat plate, or around blunt or streamlined bodies, as for example the case of ship hulls.

Several investigators have observed, in the laboratory, reductions in viscous drag of up to 50 percent but as yet are still unable to determine the exact mechanism by which the drag is reduced. This phenomena of drag reduction has been observed for concentrations of polymer solutions which were sufficiently low (between 10 to 100 weight parts per million parts of water) so that the solution for all practical purposes retains the properties of the solvent. This, to some extent, depends on the polymer type since some exhibit non-Newtonian characteristics at even 1 wppm, whereas, others have only slight property changes at low concentrations.

At present, low concentration polymer solutions are being used to reduce the drag in the pumping over long distances of oils, water, and other liquids.

Further, it is hoped that, when better analytic or experimental methods are available to predict the effects of long chain polymers on boundary layer flow, polymer solutions will prove to be a feasible way to reduce the drag on submarines or surface vessels. For merchant vessels this feasibility would entail a lowering of the transport costs, whereas for naval craft it could mean a higher maximum speed and/or larger cruising distances.

This thesis is one of a continuing set of investigations being conducted in this laboratory into the field of liquid boundary layer phenomena and presents the results of an experimental study of the boundary layer formed on a flat plate situated in a free surface water channel. The flat plate was subjected to flows of homogeneous polyacrylamide solutions with concentrations from 0 to 75 parts per million by weight.

Velocity profiles were obtained at a large number of positions along the plate in order to determine the effect of polymer additives on the velocity distribution, growth and other boundary layer parameters, and also to correlate the drag predicted using the velocity distribution with direct drag measurements.

CHAPTER II

LITERATURE SURVEY:

The use of long-chain polymers to reduce the viscous drag on bodies has been under investigation for the last twenty years.

In 1948, Toms (1)* observed that the flow rates in turbulent pipe flow of monochlorbenzene could be greatly increased by dissolving in the monochlorbenzene small accounts of polymethyl-methaccylate. He attributed these results to the wall effects put forward by Oldroyd (2), who suggested that in the immediate neighbourhood of a solid wall, a preferred direction could be introduced into a normally isotropic fluid and in the case of these polymers, an abnormally mobile laminar sublayer might exist and produce an apparent velocity of slip and hence an increase in the flow rate. During his experiments, Toms found that up to a 50 percent reduction in turbulent viscous drag could be achieved.

Numerous subsequent measurements have confirmed Toms' discovery and have generalized it to include the peculiar behavior observed in the turbulent flow of all high molecular weight polymer solutions past walls.

A thorough theoretical analysis of the turbulent flow of non-elastic, time independent, power law fluids was given by Dodge and Metzner (3). They performed experiments using Carbopol,

---

* (Numbers indicate references in reference list).

sodium carboxymethy cellulose (CMC), slurries of attasol and attapulgite clay which verified the original analysis. It can be fairly well concluded that the general flow phenomena of the pseudoplastic, time independent, purely viscous fluids have been solved. However, in their experiments, Dodge et al. noticed that the friction factor obtained from the solutions of CMC did not agree with their theory. They attributed this deviation to the fact that the CMC possessed visco-elastic properties while the other solutions tested were truly viscous liquids.

White (4), in 1962, found from pipe flow experiments with Guar gum solutions in various concentrations, that drag reduction occurs only above a certain threshold Reynolds number which depends on the pipe diameter. Below this critical value of Reynolds number the fluid exhibits normal Newtonian behavior.

Elata and Tirosh (5) put forward another correlation based on the results of their drag reduction experiments using dilute aqueous guar gum solutions. For various concentrations, their data, when plotted on a graph of $1/\ C_f$ versus $\ln(Re_d\ C_f)$, gave a family of straight lines, and since the slope of such a straight line for a Newtonian liquid is supposed to be inversely proportional to Prandtl's mixing length constant "k", they concluded that "k" was no longer a universal constant. Meyer (6) re-evaluated their work and pointed out that the constant "k" had not changed and that the variation in the slopes was due to a thickening of the laminar and buffer layers near the wall.

Hershey (7) explained the drag reduction phenomena by the concept of relaxation times of the polymer solutions. When a Newtonian polymer solution is flowing turbulently, a typical Newtonian friction factor behavior would be observed, provided the relaxation times of the major portion of the polymer molecules are small compared with a time scale characteristic of the flow. If the latter value was smaller, high frequency eddies would transform into low frequency eddies before relaxation could occur. The energy dissipated would then be lower and thus cause turbulence suppression and drag reduction.

Furthermore, Pruit and Crawford (8) found that for turbulent flow in pipes, increased molecular weight, within any homologous polymer series, increases the drag reducing efficiency of the polymer.

Love (9) conducted an experimental investigation into the effects of injecting non-Newtonian fluids into the turbulent boundary layer formed on a flat plate. The drag on the plate was obtained by computing a momentum balance across a plane in the wake, normal to the free stream flow direction, using a velocity profile at that plane. The ejection of weakly visco-elastic solutions of a macromolecular polymer at the leading edge of the plate decreased its drag coefficient by as much as 50 percent. It was found that, for a given ejection rate and free stream velocity, there was a solution concentration for which the drag coefficient was a minimum. He conjectured that the relatively sharp loss of effectiveness for high concentrations may have been due to insufficient mixing of the additive into the turbulent boundary layer.

Love showed that ejection of neutrally bouyant spherical particles, approximately the size of the macromolecules, had no effect on the drag of the plate, thus indicating that the drag reduction is probably associated with the visco-elastic properties of the solutions studied.

Emerson (10) tested ship models in a towing tank having a dilute aqueous polymer solution in it. He reported substantial viscous drag reduction with concentrations between 10 and 100 parts per million.

Dove (11), in 1966, tested a ship model with injection through 90° slots in the sides of the model and confirmed that drag reductions can be obtained when the additive is injected directly into the boundary layer.

Kowalski (12) tested the effect of injecting additives on the frictional resistance of a flat plate, and also two ship models. Polymer solutions were injected into the boundary layers of a torpedo shaped body and a 19 foot motor boat. A drag reduction of 30 percent was observed for the former while the latter experienced at 10 percent decrease in drag.

Meyer (6), in 1966, obtained an equation which satisfactorily correlated existing data for the frictional characteristics of the turbulent flow of a dilute, visco-elastic non-Newtonian fluid in a pipe. The equation included two parameters which were characteristic of the visco-elastic fluid, one of which was strongly dependent on both polymer solute and concentration and the other appeared to be constant, and independent of the polymer solutes which were used for the research recorded in the report.

Meyer found that the data could be presented in the form of a universal logarithmic velocity profile, the turbulent portion of which could be expressed mathematically in the form,

$$\frac{u}{U^*} = A \log \left(\frac{yU^*}{\nu}\right) + B$$

which for Newtonian fluids was given as

$$A = 2.303/k = 5.77$$

and $B = 5.5$

The effect of non-Newtonian additives was found only to change the value of B. This lead Meyer to assume that the laminar sublayer had been made less sensitive to disturbances in the fluid above it and thus it becomes thicker.

Smallman (13) performed experiments on a disc rotating in aqueous polymer solutions. He found that drag reduction caused by increasing concentrations of polymer reaches a maximum, and reported that for polyacrylamides MRL-159 and MRL-295* this point is reached when the concentration is between 100 to 200

---

* (Manufactured by Stein-Hall Limited).

parts per million, and he observed that at these concentrations even the most precise viscometer (operating in the laminar regime) fails to indicate any significant change in viscosity as compared to that for water.

On the basis of his work, Smallman felt that the theory which best explained the drag reduction phenomena was the Turbulence Suppression Theory which may be stated as:

> "in any flow pattern taking place in a fluid to which has been added certain polymers in trace quantities, the flow characteristics of the fluid will be unchanged in the laminar flow regime, but the eddies occurring in the turbulent flow regime will tend to be suppressed. The flow in the turbulent regime will therefore tend to dissipate less energy than was the case before the addition of the polymers."

Sherman (14) correlated data on drag reduction in a pipe flow influenced by four types of polyethylene oxide and two types of polyacrylamide. He found that the drag reduction could be predicted knowing the molecular weight, the molecular structure, and the concentration of the solution. He also found that, at a given Reynolds number, the drag reducing effect increases with concentration to a maximum and decreases for higher concentrations. The concentration required for the maximum effect was proportional to the polymer molecular weight. He found that a generalized curve could be obtained by plotting fractional drag against the product of concentration and the effective molecular length to diameter ratio.

Kowalski (15), in a second paper, investigated the practical use of so-called non-Newtonian additives in reducing drag on full size ships with the aim of reducing the quantities of additives which were previously thought necessary. He performed tests on the effect of the angle of injection, the effect of pulsing the injection, and on the effect of the polymers on the microscale of turbulence. The character of the turbulence was observed to change from a small amplitude (high wave number) to larger amplitude (low wave number) turbulent velocity fluctuations, with the introduction of polymer.

Kowalski suggested that the change in turbulent viscous drag was due to a shift from high frequency dissipative eddies to lower frequency predominately energy conserving eddies and due to an increase in the viscous sublayer thickness causing a reduction in velocity gradient at the wall and thereby a lower shear stress at the boundary. He also noted a persistence effect in which the effect of the polymer on the flow lasted a considerable length of time after injection ceased. An injection of one second duration followed by a ten second pause was almost as effective as continuous injection. He hypothesized that if the boundary is saturated with polymer, the time required for the polymer to be washed off the surface would account for the persistence effect and slip may occur which also reduces the drag. Furthermore, injecting the polymer almost parallel to the surface was found to be about 10 times as effective as injecting normal to the wall.

On the basis of his research Kowalski felt that by combining parallel injection and a pulsing technique, 195 pounds per hour of polymer could reduce the drag on a submarine by a very significant amount.

Goren and Norbury (16) correlated information, between 1964 and 1967, on the frictional drag, velocity distribution, and concentration distribution based on Reynolds number and polymer concentration level for fully developed turbulent flow in a 2 inch diameter pipe.

They obtained a maximum drag reduction of 71 percent at a Reynolds number of 1.5×10^5 for solutions having a polymer concentration of 10 weight parts per million. For higher concentrations the drag reduction was found to be smaller. The drag reduction effect occurred only above some "critical" Reynolds number which was independent of concentration. They also found that the polymer additives influenced the flow, as shown by altered velocity profiles, only in the neighbourhood of a solid wall.

White (17) proposed a correlation for flat plates based on Meyer's (6) work for pipes. White assumed that Meyer's equation in the form

$$\frac{u}{U^*} = \frac{1}{k} \ln \left(\frac{yU^*}{\nu}\right) + 5.5 + \alpha \ln \left(\frac{U^*}{U_o^*}\right)$$

(where the subscript o represents the Newtonian case) holds for the boundary layer on a flat plate. When $\alpha = o$ the profile is that of a Newtonian fluid. From his analysis White gives the interpretation that the local skin friction coefficient on a flat plate with polymer additive is equal to the Newtonian skin friction coefficient evaluated at an effective Reynolds number R_N, given by,

$$R_N = Re\left(\frac{U^*}{U_o^*}\right)^{k\alpha}$$

This same relation was also found to hold for pipe flow. However, in applying this "effective Reynolds number" concept, external flows behave differently to internal flows because of the different manner in which U* varies with the Reynolds number. For flow in a pipe, U* increases with Reynolds number, so that the polymer causes a skin friction reduction at large Reynolds numbers. On the other hand, for flow over a flat plate U* decreases with Re_x, since U_1 remains approximately constant, hence the polymer reduces plate friction only at low turbulent Reynolds numbers and the effect will not be noticed above some threshold Re_x.

Kowalski (18) presented a review of his work in January 1968 and gave the following conclusions on turbulence within the boundary layer region. He stated that; "When a polymer is injected

i) the energy spectra shifts towards lower frequencies, away from the dissipative end and towards the conservative end of the spectrum.

ii) microscale turbulent eddies are suppressed and large eddies are enhanced. Since small eddies are responsible for conversion of energy into heat losses, dissipation of energy into heat is reduced.

iii) transport of turbulent momentum is reduced cutting down on the energy loss from the boundary.

iv) velocity profiles become less steep at the boundary resulting in a lower wall shear stress."

Latto (19) on further analysis of the work of Shen (20), also found that the velocity profiles on a flat plate with polymer injection obey the universal logarithmic profile law in the form,

$$\frac{u}{U^*} = A \log \left(\frac{yU^*}{\nu}\right) + B$$

with the effect of the polymer being to increase the value of B, thereby appearing to show an increase in the thickness of the buffer and/or viscous sublayer. They also concluded that the injection angle and injection velocity play an important role in the effectiveness of a given polymer solution.

Virk et al (21) examined the phenomena of onset of drag reduction in pipe flow and found that there appears to be a critical wall shear stress below which a polymer solution behaves essentially as a Newtonian fluid and drag reduction is not observed. They embodied this finding into the form of a critical wave number, $W_c = U^*_c/\nu$, which they evaluated as 470 and $530 \frac{1}{cm}$, for two different sets of pipe flow data for aqueous solutions of a polyacrylamide with a molecular weight of about 2.5 10^6. It was found that within any homologous series of a polymer the critical wave number varies as the inverse of the sqare root of the molecular weight.

White (22) proposed a method of determining the critical wall shear stress by plotting the wall shear stress of a polymer solution against the wall shear stress for the solvent alone, where both values are evaluated for equal boundary layer thicknesses. A logarithmic plot of these values results in two regimes which are both described by a straight line. Below the critical wall shear stress τ_0 , the wall shear for the polymer solution is equal to that of the solvent. Above this critical value the results may be described by an eqation of the form,

$$\frac{\tau_{0_p}}{\tau_{0_c}} = \left(\frac{\tau_{0_s}}{\tau_{0_c}}\right)^N$$

where N is an exponent which depends on the polymer, type of solvent and concentration.

CHAPTER III

EXPERIMENTAL APPARATUS:

1. The Flow System

The flow conditions were set up in a tilting flume which was part of a recirculating flow system (Fig. 1). A built-in concrete reservoir beneath floor level served as a sump. The maximum capacity of this reservoir is about 1900 cubic feet. A single stage centrifugal pump*, driven by a three-phase, a.c. motor+ is used to pump the water from the sump to a constant head tank located about 10 feet above the flume. A mesh screen serves as a filter to stop foreign matter from entering the flume from the head tank. At the entrance to the channel a honeycomb filter was used to align the flow, and as far as possible, reduce the free stream turbulence in the test section. After discharging through the flume, the water is returned to the sump via a drainage channel built into the floor. Another filter was incorporated into this channel to prevent debris from entering the sump.

2. The Tilting Flume

The flume itself is 30 feet long with a rectangular cross-section 12 inches wide and a maximum allowable fluid depth of 18 inches (Fig. 2). It has a 10 foot convergent section

---

* Canada Pumps Ltd. 1400 U.S. gal/min., 1150 r.p.m., 20 ft. head, 10 H.P.

\+ Robbins and Meyers Co. 3ϕ, 55V, 11A, 1140 r.p.m. 10 H.P. continuous duty.

upstream of the flume which receives water from the constant head tank. The flume is hinged at the upstream end and is supported mid way along its length by an adjustable jack which allows the flume to be tilted with respect to horizontal.

The side walls of the channel are made of 1/4 inch thick glass to allow visual observation of, and optical measurements on the flow in the channel. Two accurately aligned rails are provided on top of the side walls for instrumentation carriages. The floor of the channel, which is solid metal, has threaded holes at one foot intervals along its centre line for insertion of measuring probes.

A valve between the head tank and receiving section of the flume controls the volumetric flow rate into the channel, while a tail gate at the downstream end of the flume controls the fluid depth.

3. The Flat Plate Model

A flat plate model (Fig.3 & 4) was designed for this experiment which consisted of two main sections, the supporting structure and the working surfaces.

The supporting structure was constructed of plexiglass and was suspended from a pair of carriages above the flume. Two guard plates were provided, one on each side of the channel, to which the flat plate model was fastened, and which served to minimize the effect on the model of the channel side wall boundary layer (Fig. 5).

The moving part of the model was constructed of brass structural members with plexiglass surfaces. The cross-section was 6 inches by 3/4 inches and the flat top and bottom surfaces were 52 inches in length. A three inch long wedge nose piece and a 1 1/2 inch wedge tail piece were provided to minimize the effects of form drag (Fig. 6).

The model was supported in the guard plates by beryllium-copper leaf spring stock with the largest moment of area in the vertical plane so as to provide support for the weight of the model (Fig. 7). However the main purpose of these "springs" was to allow movement in the longitudinal direction while acting as springs in this direction. A Schaevitz Engineering Company, limited differential variable transformer (LDVT) was installed between the tail section and the solid supporting structure to measure displacements of the model with respect to the support in the longitudinal direction. The combination of this displacement transducer and the spring effect of the beryllium-copper support system provided an absolute method of measuring drag.

At 2 inch intervals along the centre line of the bottom of the plate 28 pressure taps were drilled which were connected by vinyl tubing to a pressure sensing apparatus.

The angle of inclination of the plate could be adjusted at the point where the structural members were connected to the travelling carriages. The plate was normally located about five inches from the bottom of the channel with its leading edge between 11 and 15 feet from the beginning of the flume.

4. Auxiliary Instrumentation

Velocity profiles were measured using the hot-film anemometer technique. The velocity sensitive probes used were manufactured by Thermo-Systems Inc., U. S. A. A constant temperature anemometer, Disa, Constant Temperature Anemometer, model 55A01, was used as a controlling unit. The output of the anemometer was fed into a Honeywell model 630S, digital voltmeter having a five figure numerical readout.

The hot-film probes were mounted through one of the threaded holes in the bottom of the channel on a vertical traversing mechanism which allowed measurements of movement in the vertical direction of 0.001 inches.

The energizing and output readout system for the drag transducer was a Schaevitz model TR-100, Carrier Amplifier Indicator. The output from this control unit was fed into a Honeywell Two-Pen Electronic 19 Lab Recorder.

The tubes from the pressure tappings were fed into a Scani-Valve Comp. $48P_3$ - 453, 48 port valve. The chosen port was routed to a Scani-Valve Comp. PDCR4, $\pm$ 0.2 PSID pressure transducer. The above mentioned Honeywell 2-pen recorder was also utilized for port identification. The readout of the pressure transducer was obtained by a Scani-Valve Comp. POCA3, P-Ducer OSC-Carrier AMP, and displayed on the previously mentioned Honeywell digital voltmeter.

CHAPTER IV

EXPERIMENTAL PROCEDURE:

1. System Preparation

It was initially necessary to completely clean the water circulation system before using it, as any contamination could affect the results. The water was drained off and then starting at the highest point all of the walls of the tanks were scrubbed with a coarse brush and then hosed down. The walls of the channel were cleaned to remove any accumulated grime. The sump was then filled with mains water which was circulated through the system for a short period. This water was then drained off to avoid the possibility of dirt, which had settled in the mains while not in use, from affecting the tests. All the surfaces of the storage tanks and channel were again washed down to insure the absence of contaminants. Finally the sump reservoir was filled again with untreated mains water.

If, at any time during the ensuing experimental work it was felt that the fluid properties could have been changed due to the presence of foreign matter or degraded polymers the above procedure was repeated.

2. Solution Preparation

The experimental work was performed using the flow of a homogeneous aqueous polymer solution through the circulating system. The polymer used was a non-ionic, high molecular weight polyacrylamide supplied by Stein-Hall Limited under the trade name Poly Hall MRL-402, and was supplied in a fine granular form.

The moisture content of the sample was determined by weighing a small quantity prior and after baking it. The baking operation consisted of placing a sample in a refractory furnace for two hours at a temperature of 220 degrees fahrenheit, the time and temperature as recommended by the manufacturer.

Knowing the base area of the sump tank, the volume contained, and therefore the weight of water could be assessed from the depth of the fluid. To this water was added a weight of polymer which would, after the effect of moisture content was determined, yield a homogeneous solution of desired concentration. The final concentrations used were 0, 25 and 50 parts of polymer per million parts of water by weight.

It was found that, apparently, the most effective method of dissolving the polymer was to finely sprinkle the powder into the water cascading from the end of the flume as it was being recirculated through the system. This appeared to eliminate the floculation effect that was observed when the polymer was added to a quiescent or even an aerated solvent which was being agitated.

3. Probe Calibration

The hot-film probes used were type No. 1212-60w general purpose probes manufactured by Thermo-Systems Inc. Since the Disa anemometer was not well matched to the power requirements for the TSI probes, an overheating ratio was chosen so that at a maximum water velocity of three feet per second the anemometer voltage output was approximately 20 volts.

It was found that variations in the water temperature had a pronounced effect on the probe characteristics which could not be compensated for, due to the fact that the Disa anemometer had only a three decade resistance variation. This problem was overcome by installing an auxiliary continuously variable potentiometer in series with the lowest decade.

The probes were calibrated in the working solution by establishing a velocity in the channel and comparing the output of the anemometer with the velocity determined by a combination of pitot probe and visual observations of the velocity of neutral density particles.

For low velocities (less than about 1.5 ft/sec) the velocity was obtained by determining the time required for neutrally bouyant particles to travel a given distance with the water flow. For higher velocities a pitot probe was used to determine the velocity. For velocities between 1 and 2 feet per second, there was close agreement between the calibration methods.

It was found that, after a period of use in the homogeneous solution, the hot-film sensor output decreased, which was apparently due to a build up of polymer molecules on the probe. However, creating a disturbance upstream in the flow, or brushing the film with a soft brush appeared to remove the molecules and the probe resumed its normal operating characteristic.

4. Drag Transducer Calibration

The drag measurement set up was calibrated while the plate was submerged in quiescent water to negate any bouyancy effect.

The drag measurement system was calibrated by applying weights to a fine thread which was passed over a frictionless pulley at the tail gate and attached to the rear end of the plate, and noting the relative displacement. This procedure was employed before and after any drag measurements were made to ensure reproducibility of the measurement system.

5. Test Procedure

By adjusting the solution flow rate and depth of solution in the channel, a free stream velocity of 2.21 ± 0.01 ft/sec was achieved in the test section.

The flat plate model was then located with its leading edge over the hot-film probe which was mounted through the bottom of the channel and a velocity profile traverse was made perpendicular to the plate. The model was then moved forward along the rails and another velocity traverse was made. The plate was moved forward a total of 34 increments of 1 1/2 inches for each solution concentration yielding data for 35 velocity profiles for each set of flow conditions. Meanwhile, the output from the displacement transducer was continually observed in order to ensure that no change had taken place in drag, which would have indicated a change in the effect of the flow media.

Initially, the pressure distribution along the plate was observed but was found to be smaller than the accuracy of the associated measuring equipment and was therefore neglected.

Normally, the temperature of the solutions varied between 79°F and 82°F during the tests. A variation of temperature inside this range had no noticeable effect on the instrumentation but if a variation outside this range occurred no results were taken.

Finally, the variation of drag with concentration and time was determined over a period of 3 days for concentrations of 0, 25, 50 and 75 wppm.

Initially, the drag with zero concentration was determined using untreated mains water. The concentration was then increased to 25 wppm and the drag was recorded over a 24 hour period. The tests were repeated using concentrations of 50 wppm and 75 wppm. These concentrations were obtained by adding more polymer to the previous solution.

CHAPTER V

PROCESSING THE EXPERIMENTAL DATA:

This discussion is limited to the methods employed to correlate the raw experimental data into a form which would show the effects of polymer on boundary layer flow.

For each value of distance x along the flat plate model a non-dimensional velocity profile, u/U_1 versus y, was drawn using the calibration curve for the hot-film probes and the output voltages from the anemometer. Typical profiles are shown in Fig. (8, 9, 10) where the station number corresponds to one of the 35 profiles taken along the plate for a given concentration.

Values of u/U_1, for 35 predetermined values of y, were punched onto Fortran compatable computer cards using a Benson-Lehner Oscar analogue to digital converter. This converter divides a preset span, in either coordinate direction, into a thousand intervals and when the axes of the instrument is placed over a point the coordinates of that point in either or both directions may be read onto a punched card. To simplify calculations and increase accuracy, predetermined values of y were chosen prior to using the converter.

Using this data, the function $(\frac{u}{U_1} - (\frac{u}{U_1})^2)$ was evaluated for the chosen values of y and numerically integrated from $\frac{u}{U_1} = 0$ to $\frac{u}{U_1} = 0.99$ using a trapezoidal approximation method to yield the momentum thickness. These determinations were performed on a computor for all stations along the plate, so that the output enabled a plot of θ versus x to be drawn. A correlation between θ and x was obtained in the form of a polynomial by making use of a least squares curve fitting subroutine on the IBM 7040 computor. Points which lay significantly further than two standard deviations from the fitted curve were discarded as being suspect and the remaining points were fitted with a polynomial. This derived function for θ is shown in Figures (8, 9, 10, 11, 12, and 13).

For a boundary layer with zero pressure gradient and U_1 is a constant, we may write the Von Karman Momentum Integral equation in the form

$$\tau_0/\rho \;=\; U_1^{\,2}\,\frac{d\theta}{dx}$$

and since

$$C_f \;=\; \frac{\tau_0}{\rho U_1^{\,2}/2}$$

then

$$C_f \;=\; 2\,\frac{d\theta}{dx}$$

and therefore the local coefficient of friction may be determined from the momentum thickness growth profiles for any value of x.

The friction velocity U^* may be expressed as

$$U^{*2} \;=\; 2\,\tau_0/\rho$$

$$=\; \frac{2\tau_0}{\rho U_1^{\,2}} \times U_1^{\,2}$$

or

$$U^* \;=\; (C_f)^{1/2} \times U_1 \,.$$

Then, the data for u/U_1, y, U_1, x and θ were entered, together with a final computer program which was used to evaluate the parameters U^+ and Y^+ in the Universal Logarithmic Velocity Profile:

$$U^+ = A \ln Y^+ + B$$

where $$U^+ = \frac{u}{U^*} .$$

U^+ is evaluated from the equation,

$$\frac{u}{U^*} = \frac{u}{U_1} \times U_1 \times \frac{1}{U^*}$$

and $$Y^+ = \frac{yU^*}{\nu}$$

These logarithmic profiles are shown in Figures (14, 15, 16).

This program was also used to determine the Reynolds number (Re_x), and using the trapezoidal approximation, the frictional drag of the plate was evaluated. The drag was calculated from the expression

$$D = \frac{\rho}{2} \int_0^L C_f \, U_1^2 \, dx.$$

The variation of C_f with Re_x for the three concentrations used is shown in Figure (17) while the variation in drag with polymer concentration is shown in Figure (18).

CHAPTER VI

DISCUSSION OF RESULTS:

It is difficult to compare the results of the experimental work reported here with that of previous researchers, since at this embryonic stage of development, very little information is available on the effects of aqueous polymer solutions on the boundary layer phenomena in external flows. Most of the published information on polymer solution flow is general and since in the majority of cases the particular conditions under which previous research was carried out are unavailable, only qualitative comparisons can be made.

1. Polymer

Some workers in this field of endeavour have made use of different types of polymers which cover a large range of molecular weights and properties. This research was performed using a poly-acrylamide Polyhall MRL-402 (a non-ionic, high molecular weight polyacrylamide, supplied by Stein-Hall Limited), since it combined the advantages of high molecular weight (of the order of 6 to 7×10^6), relative stability and a comparatively large solubility in water. This type of polymer was also chosen in consideration of future research since it is felt that the polyacrylamides are one of the few types of polymer presently available which may be analysed by gel permiation chromotographic or electron microscopic techniques and whose properties and molecular distribution may be reproducible from one batch to another.

2. Degradation

At the beginning of the research it was feared that degradation of the polymer solution may present a definite problem. Very little is known about degradation of polymers at present but researchers have felt that any or all of the following factors may promote degradation; aging, mechanical shear, or chemical or bacterial action. There was no reasonably simple method of simulating the effects of degradation equivalent to the degrading forces in the flow system. However, it is felt that no appreciable degradation occurred during each test. One solution was used over a period of one week and the data taken at the end of the week agreed well with the results taken five days earlier. Since this was the longest period over which a solution was used before the tanks were cleaned and a new solution made, it may be safely assumed that degradation was not an important factor. Also in the tests in which drag readings were continuously recorded over a 24 hour period, the directly measured drag did not change a noticeable amount.

3. Velocity Profiles

The major analysis of this report is based on the velocity profiles taken in the boundary layer and therefore, measurement of the hot-film probe position and anemometer output were of the utmost importance.

The output of the anemometer was fed to a Honeywell 5 figure display, digital integrating voltmeter which was set to integrate over a one second period. The variation in this voltage reading was observed until the output could be evaluated to the fourth figure. This output was always greater than ten volts with an uncertainty of the order of 0.05 volts and this would infer a maximum error of $\pm$1/2% in the voltage. In converting this voltage to velocity by using the calibration curve for the probe the maximum error in the velocity would not exceed 1.5%. There was also difficulty in determining the position of the hot film sensor. The sensor supports could be made to just touch the flat plate surface by observing the mirror image of the probe, which resulted in a small gap between the sensor element and the plate. This small but finite distance was estimated using the sensor diameter (0.006 inches) as a comparison and appeared to be approximately 0.002 inches which meant that the hot-film centre line was about a minimum of 0.005 inches from the plate. However, due to the effect of the solid surface at this close proximity to the plate, the velocity determination could not be ascertained with any accuracy and therefore a large error in the profile in the viscous sublayer could have been incurred. At larger distances from the plate the solid surface was assumed to have a negligible effect on the performance of the hot film probe.

Typical developing velocity profiles for the three concentrations 0, 25 and 50 wppm are shown in Figures (8, 9, 10). It is noticed that the profiles for a polymer solution have a larger boundary layer thickness and a lower velocity gradient at the wall than for pure water which would suggest a lower skin friction coefficient.

It is generally agreed that the constant A in the logarithmic law equation, $U^+ = A \ln Y^+ + B$, is reasonably universal at a value of about 2.50. However values for the constant B have been reported varying between 3.7 and 5.5 for pure water. The value for B obtained in this research is 3.43 (Fig. 14). For a 25 wppm polymer solution, the value of B is increased to 4.55, Fig. (15).

The variation in the values of B for pure water may reflect on the water used in the determination as any foreign matter would tend to change the flow structure. Since a standard procedure has been used in this experimental work and the water used is from one source, it may be assumed that the change in the value of B is due solely to the effects of the polymer on the flow phenomena.

Comparing the universal logarithmic profiles for pure water and the 25 wppm aqueous polymer solution, the qualitative results are as expected. The value of A is approximately 2.50 in both cases and the increase of the value of B with the addition of polymer to the water appears to indicate an increase in the thickness of the laminar sublayer. This is in agreement with the deductions of previous investigators such as Meyer (6), White (17) and Latto (19). However, when the logarithmic profile for the 50 wppm solution is examined, a marked deviation from what might be expected occurs, Fig. (16). A single curve is no longer sufficient to describe the profile. It appears that for each value of x it may be possible to draw a straight line through the data. From the graph, it is apparent that the slopes of any of these lines are much greater than the slope obtained for untreated water or the 25 wppm polymer solution. It also appears that the further along the plate in direction of flow (station 1 is at the leading edge, 35 at the trailing edge) the larger the value of B for the 50 wppm aqueous polymer solution.

Kowalski (23) observed a similar behavior for high concentration injected flows. His experiments consisted of ejecting polymer solution from the nose piece of a flat plate into the boundary layer. He explained the difference in the profiles as being the result of diffusion of the polymer solution into the free stream. For the injection of large concentration solutions, the solution would diffuse into the free stream and thus concentration gradients would be established both normal and parallel to the main flow. Therefore, each profile would be representative of different concentrations and concentration gradients and would not be expected to give a universal profile. The data of Latto (19) shows this same tendency for high concentration injected flows.

The data for this research was taken for a homogeneous aqueous polymer solution and consequently, this argument would not appear to apply. The persistance effect which Kowalski (15) postulated may possibly explain some of the results of this report. That is, if the polymer was attracted to the plate surface a larger concentration of polymer may accumulate near the plate which would lead to a polymer concentration gradient near the surface. This attraction may possibly be due to electrostatic charges on the flat plate model and a polarizing tendency of the polymer molecule. This electrostatic attraction could well describe the persistance effect reported by Kowalski.

4. Momentum Thickness and Drag

The growth in the momentum thickness is shown in Figures (8 to 13). The momentum thickness for the 25 wppm polymer solution when compared to that for water is larger for low values of x but the growth curves cross at some value of x. The momentum thickness for the 50 wppm solution, however, is always greater than for pure water. This phenomena was also observed by Latto (19) in his report on injected flows. He noticed the tendency for the momentum thickness to be larger at low values of x than for pure water and that the greater the amount of polymer injected the larger the momentum thickness. These momentum growth profiles for the polymer solution never crossed each other but all had a tendency to cross the curve for pure water at some large value of x.

The data for the 25 wppm solution are not significantly different, in a statistical sense, from that of water, having between a 10 and 15% chance of the difference between the two being due to random errors (see Appendix II). However, the data for the 50 wppm solution are found to be significantly different from that of water.

Of more importance, however, is the slope of the momentum thickness profile which is directly proportional to the local coefficient of drag. The relationship between C_f and Re_x is shown in Figure (17). It can be seen that the local coefficient of skin friction for the 25 wppm solution is predominantly lower than that for water but converges as Re_x is increased. This is in agreement with the work of others who have noticed that there is a critical Reynolds number above which no drag reduction is felt.

The C_f curve for the 50 wppm solution is different from what might be expected; the values for this concentration being predominantly larger than the case for untreated water. The measurements for this particular concentration were repeated using a different type of hot film probe and the results of both runs were in agreement. It must therefore be assumed that the results indicate the actual characteristics of the flow. An explanation of this will be attempted in a later paragraph.

The directly measured total drag as a function of concentration is shown in Figure (18) and the form of the curve is as expected; the drag reduces as the concentration of the polymer is increased until a limit of drag reduction is reached and thereafter the drag increases above the minimum value, as the amount of polymer in solution is increased. The drag due to viscous shear, as calculated from the skin friction curves (Figure 17) is compared to the total drag in the following table.

CONCENTRATION (wppm)	SKIN FRICTION DRAG (lb_f)	DIRECTLY MEASURED TOTAL DRAG (lb_f)	APPARENT PROFILE DRAG (lb_f)
0	0.082	0.110	0.028
25	0.083	0.088	0.006
50	0.114	0.072	-0.042

The drag variation with concentration obtained from the velocity profiles does not show the same behaviour as that obtained by direct measurement. As the concentration is increased, the viscous drag calculated from the velocity profile data becomes a larger portion of the total drag, and at 50 wppm the calculated viscous drag is larger than the directly measured drag.

From the above, it can be seen that the measured total drag relationship appears to be in complete agreement with that obtained by previous researchers. However, the variation of the velocity profiles and their dependent algebraic parameters, the momentum thickness, the skin friction coefficient and integrated drag do not behave as would be expected, but no other data are apparently available to make comparisons with.

All bodies of finite thickness experience eddy shedding when subjected to the flow of a real fluid which results in profile drag on the body. The introduction of polymer into the fluid apparently tends to decrease the loss of energy in turbulent eddies. Thus, if the energy lost due to eddy shedding is reduced by the presence of polymer in the flow a net reduction in profile drag will result. This phenomena most likely accounts for the reduction in the total drag that has been observed.

5. Critical Wall Shear Stress

A logarithmic plot of wall shear stress for the 25 wppm polymer solution versus the wall shear stress for the solvent alone, as put forward by White (22) is shown in Figure (19). It is seen that the curve has two regions. At low values of wall shear the value for the polymer solution is identical to the value for the solvent. Above the so-called critical wall shear stress τ_{0_c}, the value of the shear stress for the polymer solution is lower than that for the solvent. The division between the two regions for this solution was found to occur at a wall shear stress of $\tau_{0_c} = 0.0111\ lb_f/ft^2$. For shear stresses above τ_{0_c}, the curve can be fitted with a relationship of the form,

$$\frac{\tau_{0_p}}{\tau_{0_c}} = \left(\frac{\tau_{0_s}}{\tau_{0_c}}\right)^N$$

and for the polyacrylamide solution of concentration 25 wppm, N is found to have a value of $N = 0.906$.

Referring to Figure (17), the value of C_f at which the 0 and 25 wppm curves cross is 0.0022 which corresponds to a critical wall shear stress of 0.0105 lb_f/ft^2, or a critical friction velocity of 0.0736 ft/sec. Expressing this friction velocity in the form of a wave number, $W_c = 7670 \frac{1}{ft} = 252 \frac{1}{cm}$. Assuming that the critical wave number, within any homologous polymer series, varies inversely as the square root of the polymer molecular weight, as proposed by Virk, the equivalent critical wave number corrected for a molecular weight of 2.50×10^6 from 10^7 has a value of $W_c = 504 \frac{1}{cm}$. This agrees favourably with the values obtained by Virk for a polyacrylamide of molecular weight 2.5×10^6, that is, 470 and 530 $\frac{1}{cm}$ for two different sets of pipe flow data.

The analysis of this thesis is based on the assumption that since the polymers are added to the water in very minute quantities the behavior of the resulting solution will be essentially that of the solvent. That is, thermo-physical properties of the solution are not appreciably different from those of pure water, and since the mass ratio of polymer to water is of the order of 5×10^{-5}, it would appear that this is a plausible assumption. It is known that aqueous polymer solutions can be visco-elastic, however the degree of visco-elasticity is somewhat dependent on the concentration. The degree of divergence from Newtonian fluid behavior and the criterion for determining the concentration at which the solution can be considered appreciably non-Newtonian are vague. Some polymers appear to exhibit visco-elastic effects in concentrations as low as 1 wppm while other polymers do not have an appreciable effect on the viscosity of the solution when dissolved in higher concentrations. Although there is no data at present available on the visco-elastic properties or the thermo-physical properties of aqueous polyacrylamide solutions, it is felt that, in light of the data obtained in this work, changes in these properties may be the key to the mechanism of drag reduction.

Since there is no evidence to the contrary, and the results of this research appear to be reproducible, the assumption that the physical properties of the solution are not significantly different from those of the solvent must be at fault. This may explain the apparent contradiction that the viscous drag, calculated from the velocity profile data, for the 50 wppm solution is larger than the total drag measured directly as well as the deviation of the log-law profiles, from the universal form that has been observed by other experimenters and is also confirmed by the 25 wppm solution. It is felt that much more research needs to be carried out on the thermo-physical properties of aqueous polymer solutions.

The results of this experimental work appear to indicate that much more work needs to be carried out in the area of reducing drag by using polymers but much promise is given for future applications. It seems that, at this stage, it is important that the microscopic behavior of the boundary layer in polymer solution flows be examined more thoroughly to gain an insight into the mechanism of drag reduction. From the experimental data, it would appear that, even though the polymer is dissolved in the water in minute quantities, it may considerably affect some of the thermo-physical properties of the solution. Unfortunately, at the time of the research there were no simple methods available for determining these properties.

Since this is apparently the first attempt at assessing the effect of polymers on external boundary layer phenomena through extensive velocity profile data, a positive contribution has been made. It has been shown that there is a critical wall shear stress which must be exceeded before polymers have any effect on viscous drag and is analogous to the onset criterion for pipe flow. At present this criterion can be determined experimentally only by the analysis of extensive data on external flows. A comparison has been made between direct total drag measurements and indirect viscous drag calculations which has inferred that the introduction of polymers into the flow effects not only the viscous drag but also the profile drag.

CHAPTER VII

CONCLUSIONS:

As a summary to the previous discussion, the following conclusions may be drawn:

1) Drag reduction was observed as expected. The maximun drag reduction was of the order of 33%, which occurred for a 50 wppm concentration of polyacrylamide with a length Reynolds number of about 1.25×10^6.

2) A critical wall shear stress, analogous to the onset shear stress in pipe flow work, was observed. For the polyacrylamide of molecular weight 10^7, this critical shear stress was determined to have a magnitude of 0.011 lb_f/ft^2. For wall shear stresses below this value, the presence of polymer has no effect on the viscous drag.

3) A critical wave number was determined which had a value of $252 \frac{1}{cm}$ for the polyacrylamide used. When corrected for the molecular weight effect, this value agreed with the values for a polyacrylamide determined by Virk (20).

4) Profile drag is apparently reduced when polymer is added to external flows due to the reduction of energy losses caused by eddy shedding.

5) The thickness of the viscous sublayer of the boundary layer is apparently increased by the addition of polymer to the flow.

6) The momentum growth profiles for aqueous polymer solutions form a family of non-intersecting curves, which intercect the solvent curve at increasing distances along the plate as the concentration is increased.

CHAPTER VIII

RECOMMENDATIONS:

One of the most noticeable observations of this experimental work is the lack of available data on the effects of the controlling variables on the results, for example temperature, polymer degradation, contamination, injection techniques, electrostatic effects, etc. Therefore, before more research of the present nature is carried out, methods of determining the thermophysical properties of the solution and the effects of the external variables on the solution should be examined. It would be extremely useful if simple methods were available for determining the concentration of the polymer, the absolute viscosity and molecular weight distribution of a given sample so that useful correlations could be made.

If more research is to be carried out, similar to this work, the author would advise the investigation of different methods of measuring velocity profiles, such as the use of laser anemometers or at least the use of different smaller hot-film probes which should yield better results in the sublayer. Also, methods of determining the local viscous shear on the surface of the plate would yield data which could be correlated with the skin friction coefficient calculated from the velocity profiles. Finally, means of attaining higher Reynolds numbers would allow a better interpretation of the data.

REFERENCES

1. Toms, B. A., Some Observations on the Flow of Linear Polymer Solutions through Straight Tubes at Large Reynolds Numbers, Proc. Int. Rheological Congress II, PP135-41, Schreveninger, Netherlands, 1948.

2. Oldroyd, J. G., ibid.

3. Shaver, R. G. and Merrill, E. W., Turbulent Flow of Pseudo Plastic Polymer Solutions in Straight Cylinder Tubes, A.I.Ch.E. Journal, Vol. 5, No. 2, June 1959, pp. 181.

4. White, A., Turbulent Drag Reduction with Polymer Additives, Journal of Mechanical Engineering Science, Vol. 8, No. 4, 1962, P. 452.

5. Elata, C. and Tirosh, J., Frictional Drag Reduction, Israel Journal of Technology, Vol. 3, No. 1, 1965, P. 1.

6. Meyer, Warren, A., A Correlation of the Frictvonal Characteristics of Turbulent-Flow of Dilute Viscoelastic Non-Newtonian Fluids in Pipes, A.I.Ch.E. Journal, Vol. 12, No. 3, May 1966, PP. 522-525.

7. Hershey, H. C., Drag Reduction in Newtonian Polymer Solutions, Ph.D. Thesis, University of Missouri at Rolla, 1965.

8. Pruit, G. T. and Crawford, H. R., Effect of Molecular Weight and Segmented Construction on the Drag Reduction of Water Soluble Polymers, The Western Company, Research Division, Report No. DTMB-1, April 1965.

9. Love, Richard H., The Effect of Ejected Polymer Solutions on the Resistance and Wake of a Flat Plate in a Water Flow, Hydronautics Incorporated, Technical Report 353-2, June 1965.

10. Emerson, A., Model Experiments Using Dilute Polymer Solutions instead of Water, Transactions N.E. Inst. Eng. Shipbuilders, 1965, 81(Pt7, May).

11. Dove, H. L., The Effect on Resistance of Polymer Additives Injected Into the Boundary Layer of a Frigate Model, A.E.W. Note, Feb. 1966.

12. Kowalski, T., Reduction of Frictional Drag by Non-Newtonian Additives, Naval Engineers Journal, April 1966.

13. Smallman, John R., The Influence on Hydrodynamic Drag of High Molecular Weight Compounds in the Turbulent Boundary Layer, M.Eng. Thesis, McMaster University, May 1967.

14. Sherman, Beryl A., Effect of Concentration and Molecular Structure on the Drag Reduction of Dilute Polymer Solutions, A.U.W.E. Tech. Note, 246/67, July 1967.

15. Kowalski, T., Turbulence Suppression and Viscous Drag Reduction by Non-Newtonian Additives, W12(1967), The Royal Institution of Naval Architects, London, England.

16. Goren, Y. and Norbury, J. F., Turbulent Flow of Dilute Aqueous Polymer Solutions, Transactions of A.S.M.E., Dec. 1967, Journal of Basic Engineering.

17. White, Frank M., Limitations on the Drag Reduction of External Bodies by Polymer Additives, A.I.A.A. 6th Aerospace Sciences Meeting, New York, January 1968, No. 68-127.

18. Kowalski, T., Higher Ship Speeds Due to Injection of Non-Newtonian Additives, Eastern Canadian Section of the Society of Naval Architects and Marine Engineers, Presented in Montreal, January 9, 1968.

19. Latto, B., Private Communication.

20. Shen, Chi-Hung, An Experimental Study of the Effects of Aqueous Polymer Solutions on a Liquid Boundary Layer, M.Eng. Thesis, McMaster University, May 1968.

21. Virk. P. S. and Merrill, E. W., The Onset of Dilute Polymer Solution Phenomena, Proceedings of the Symposium on Viscous Drag Reduction, held at the LTV Research Centre, Dallas, Texas, September, 1968.

22. White, D. A., The Flow of a Dilute Polymer Solution in a Turbulent Boundary Layer on a Flat Plate, Proceedings of the Symposium on Viscous Drag Reduction, held at the LTV Research Centre, Dallas, Texas, September, 1968.

23. Kowalski, T., Private Communication.

FIGURES

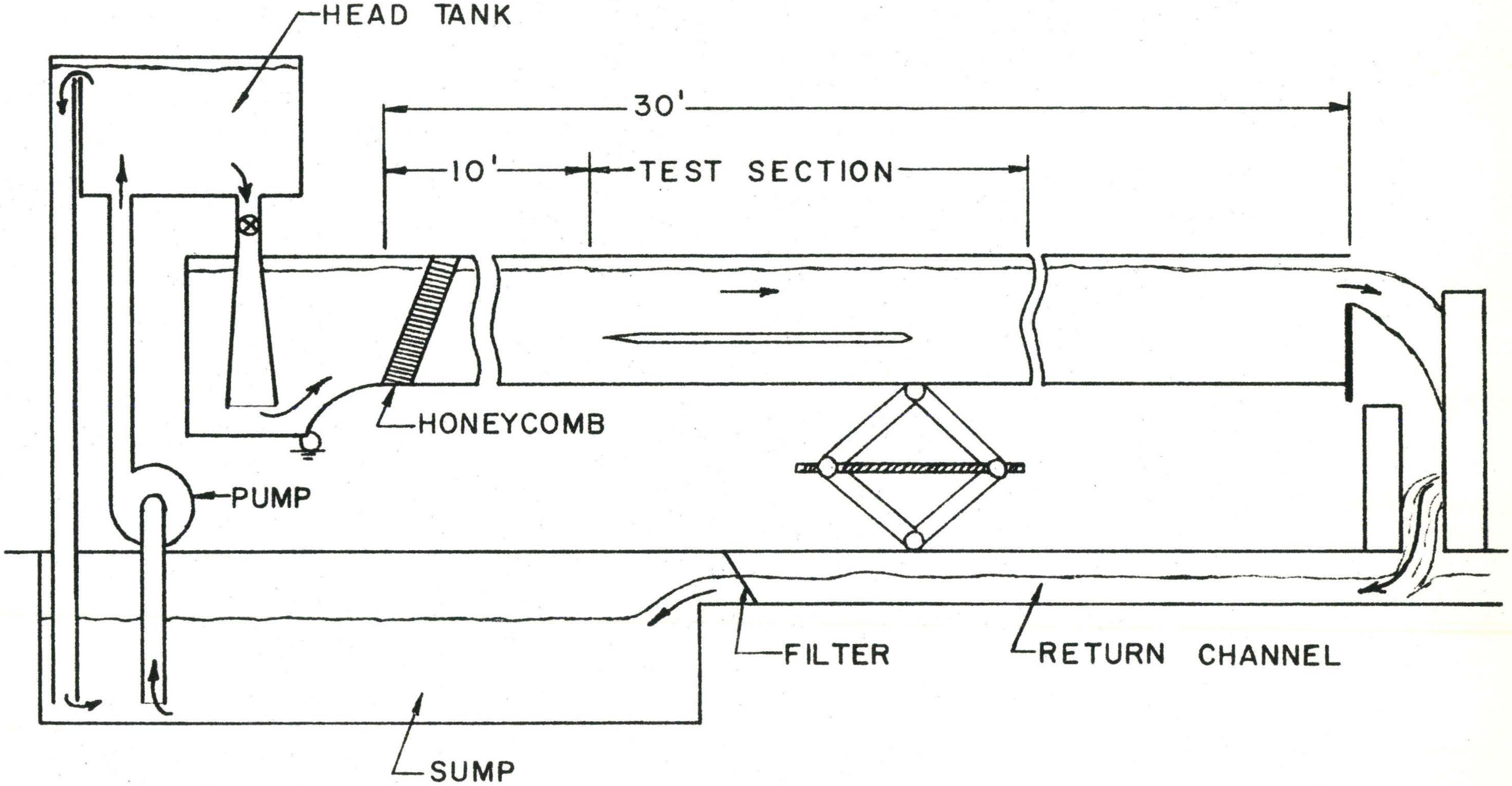

RECIRCULATING FLOW
SYSTEM
FIGURE 1

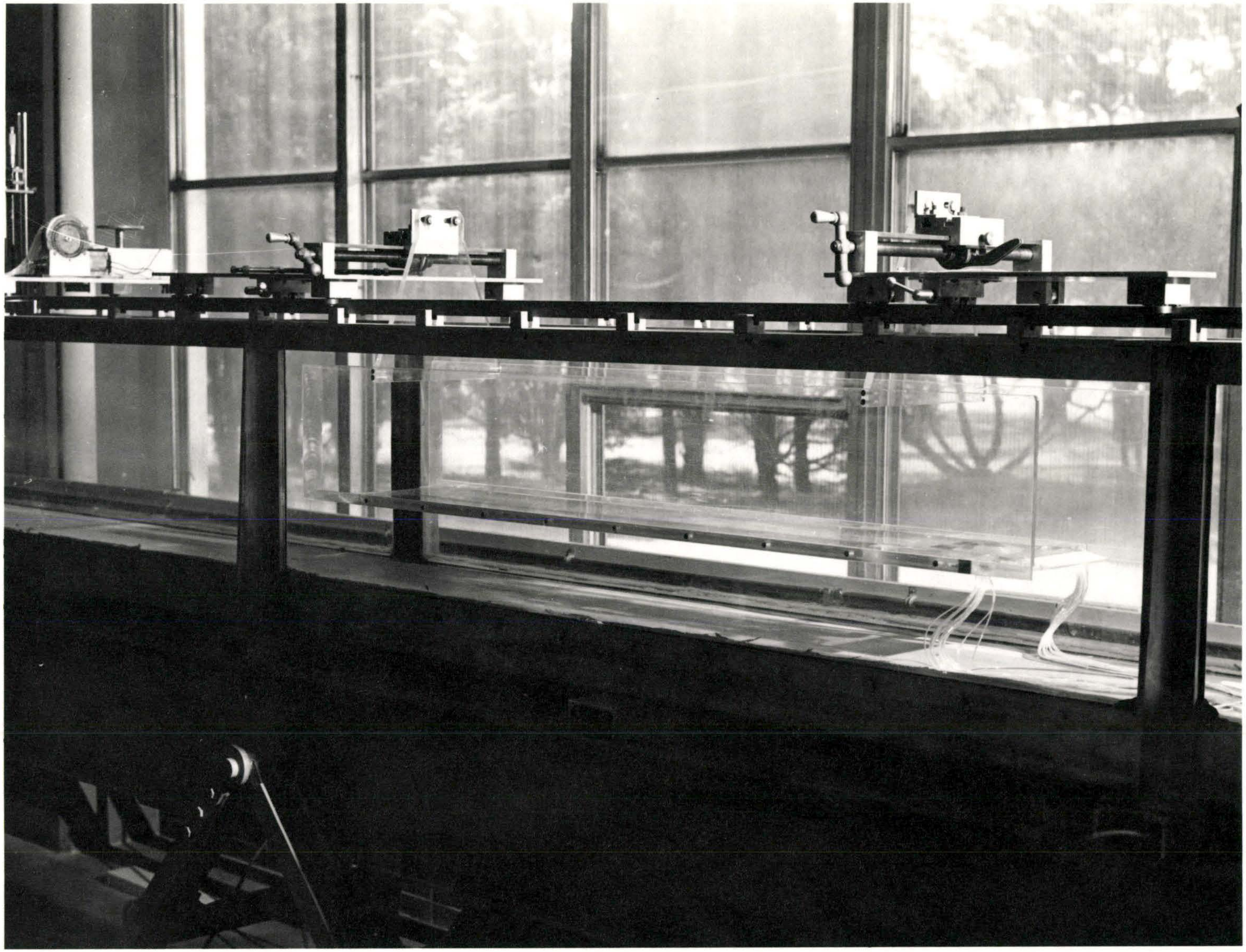

FIGURE 2 FLUME TEST SECTION

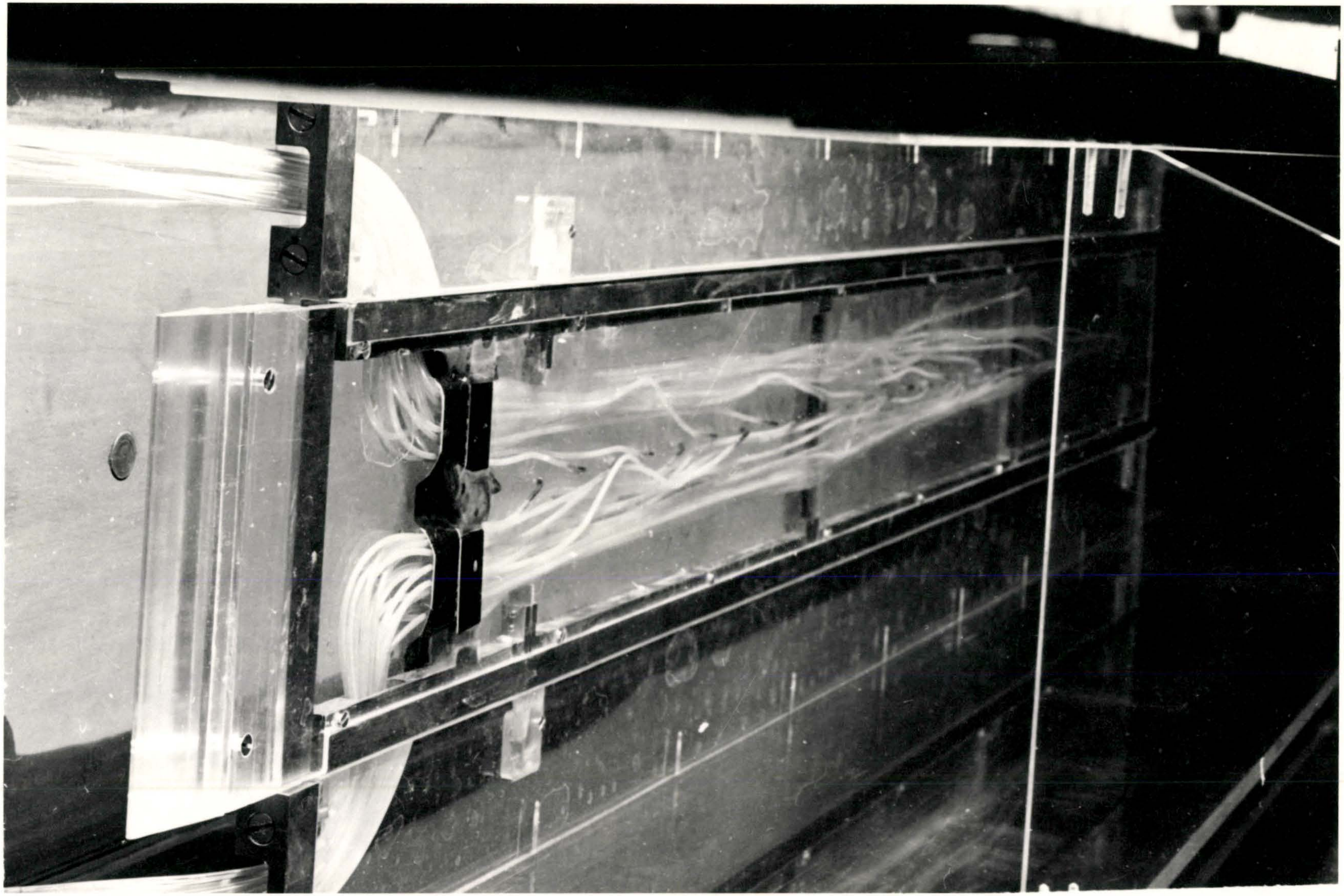

FIGURE 3 REAR VIEW OF MODEL IN FLUME

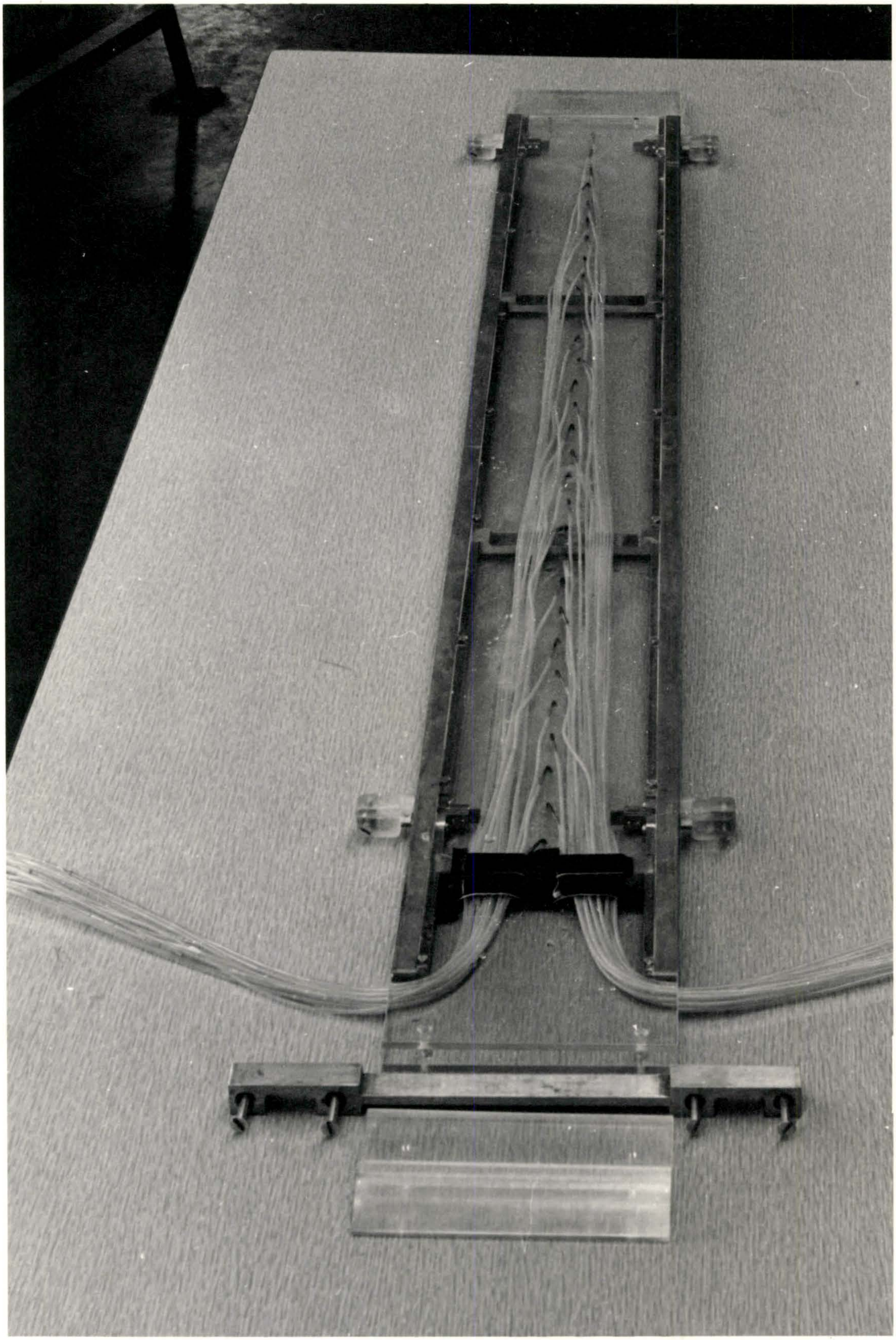

FIGURE 4 MODEL WORKING SECTION

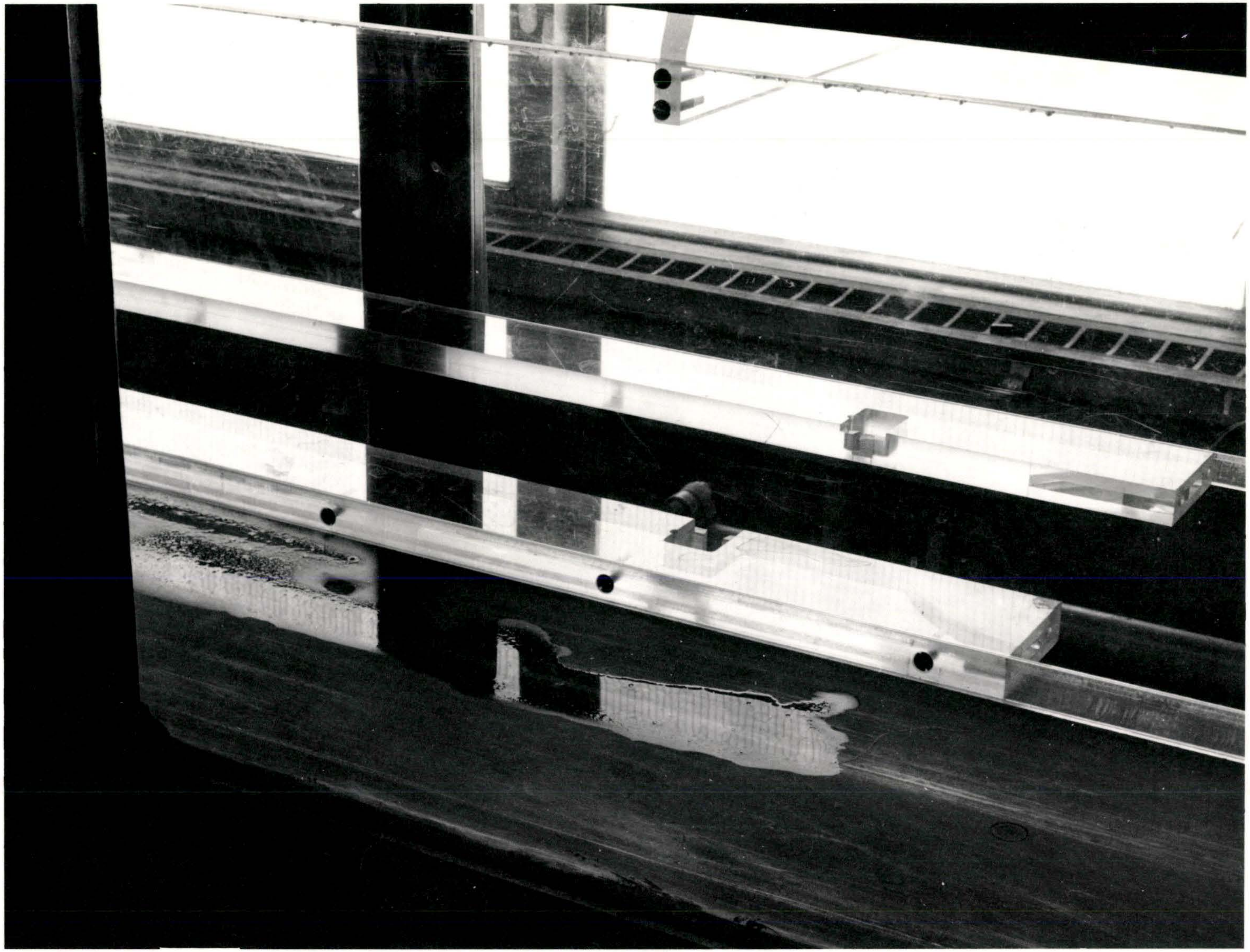

FIGUR E 5 GUARD PLATES (working section removed)

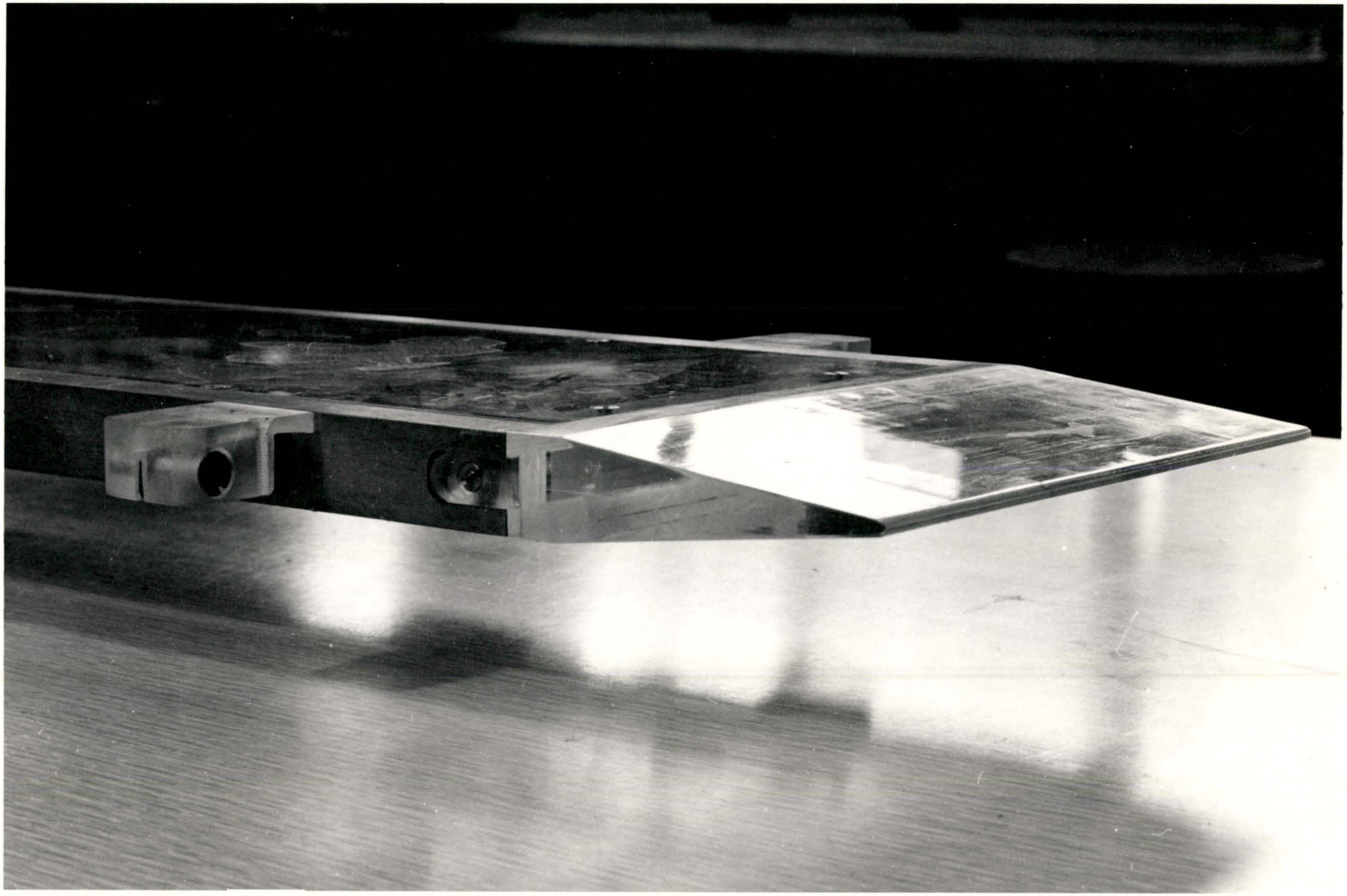

FIGURE 6 NOSE PIECE

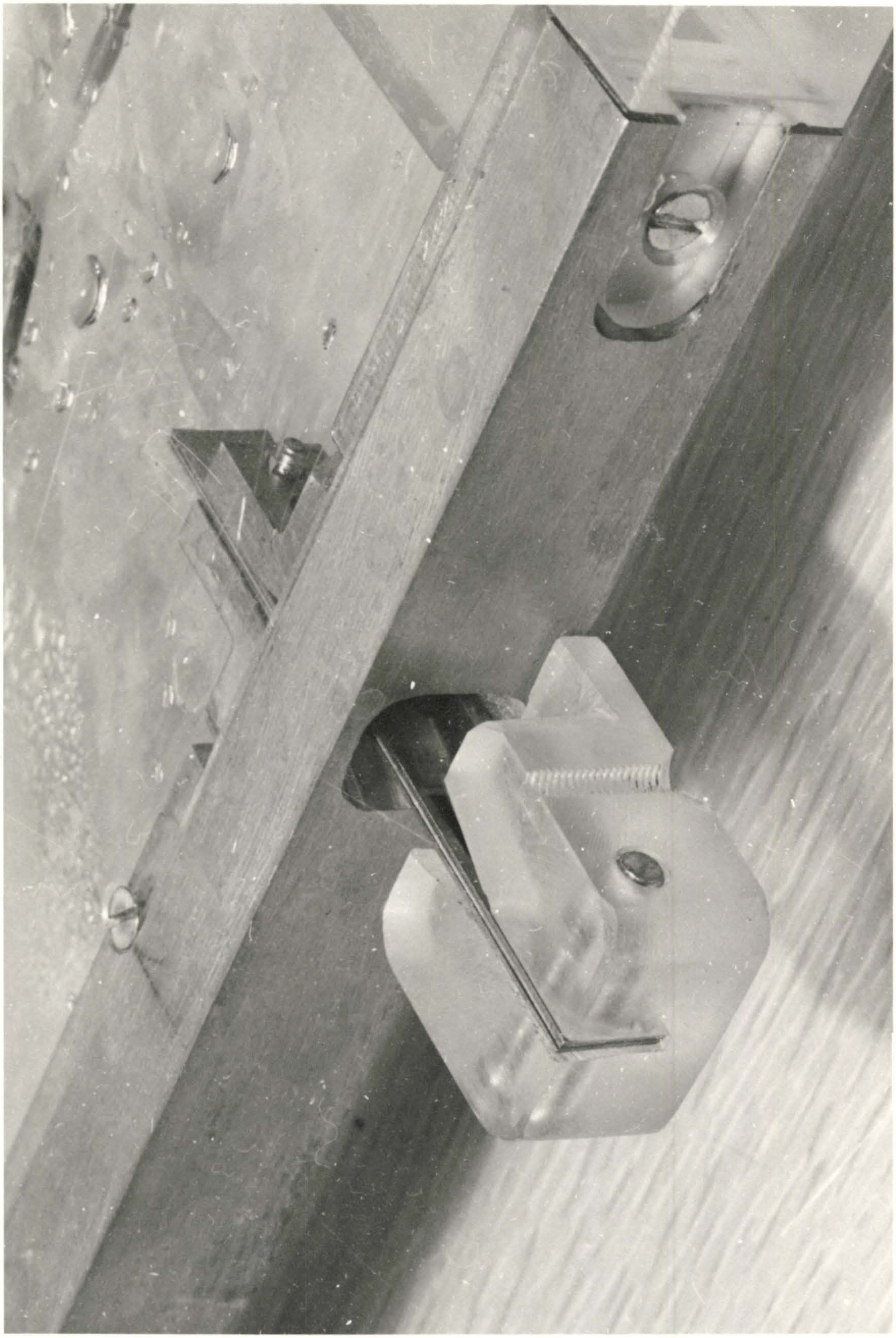

FIGURE 7 LEAF SPRING SUPPORT

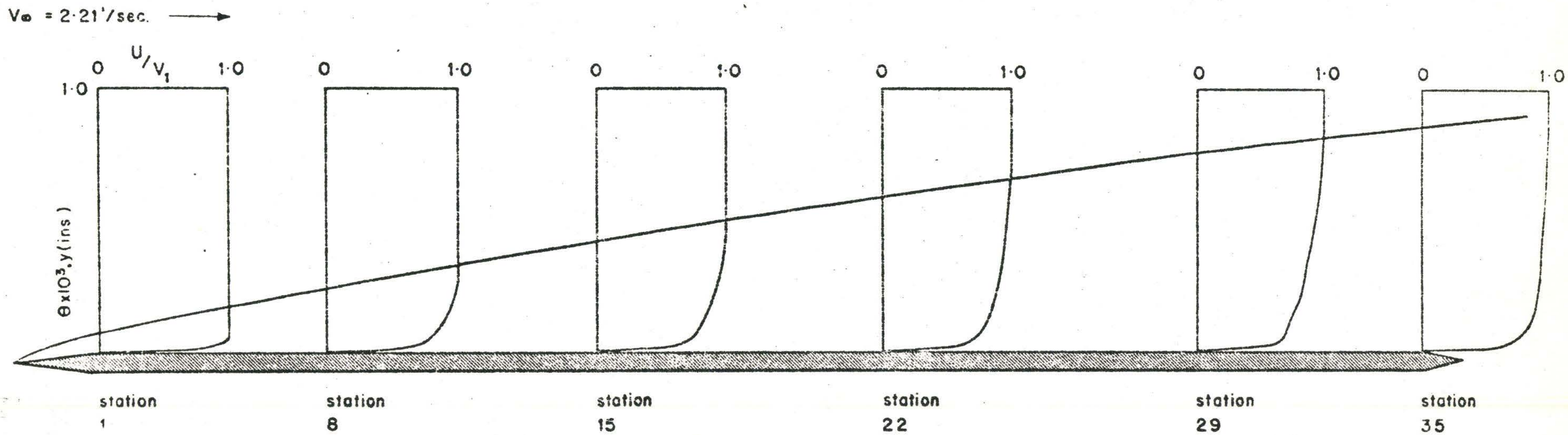

FIGURE 8 DATA FOR PURE WATER

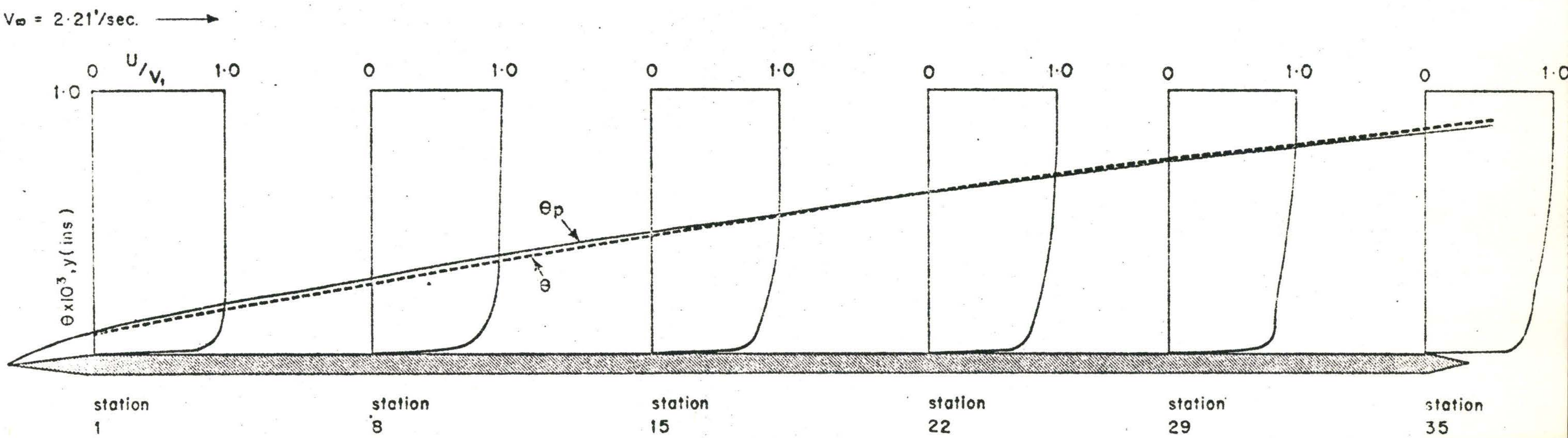

FIGURE 9 DATA FOR A 25 w.p.p.m. CONCENTRATION HOMOGENEOUS POLYMER SOLUTION

LEGEND

θ_p = momentum thickness for polymer solution

θ = momentum thickness for water

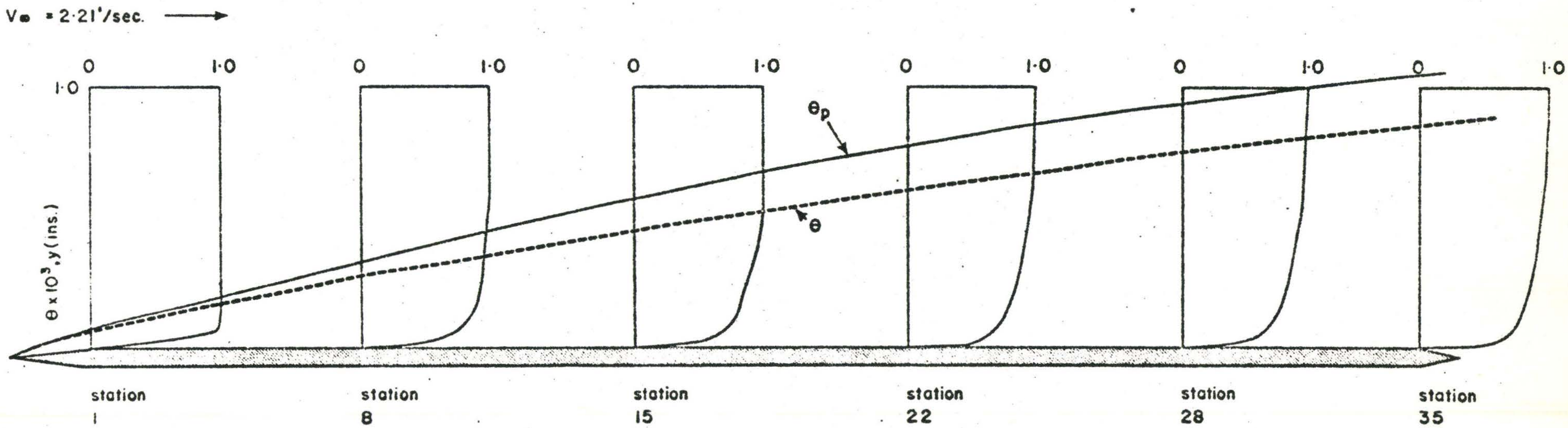

FIGURE 10 DATA FOR A 50 w.p.p.m. CONCENTRATION HOMOGENEOUS POLYMER SOLUTION

LEGEND

θ_p = momentum thickness for polymer solution

θ = momentum thickness for water

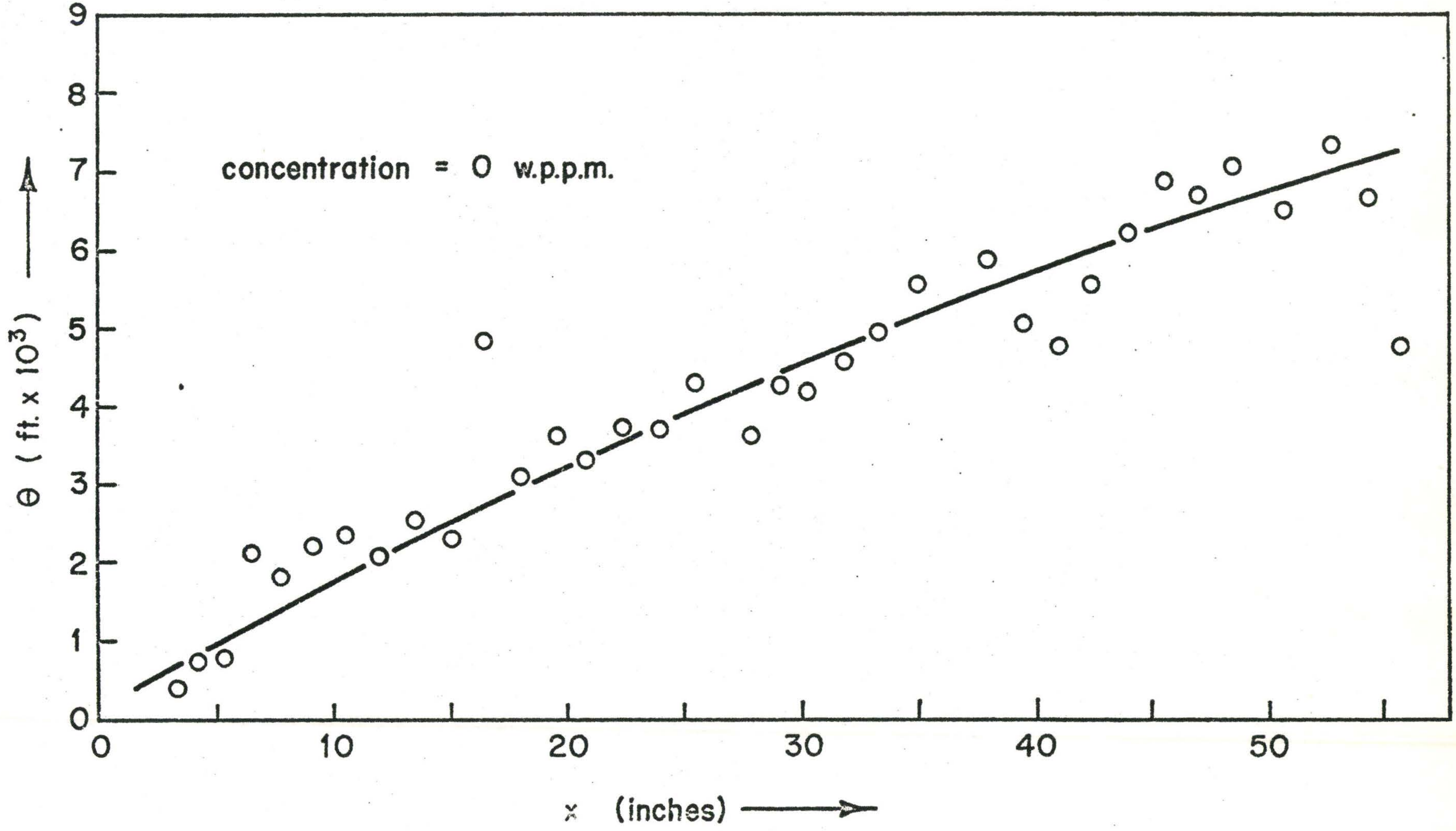

MOMENTUM THICKNESS vs X

FIGURE 11

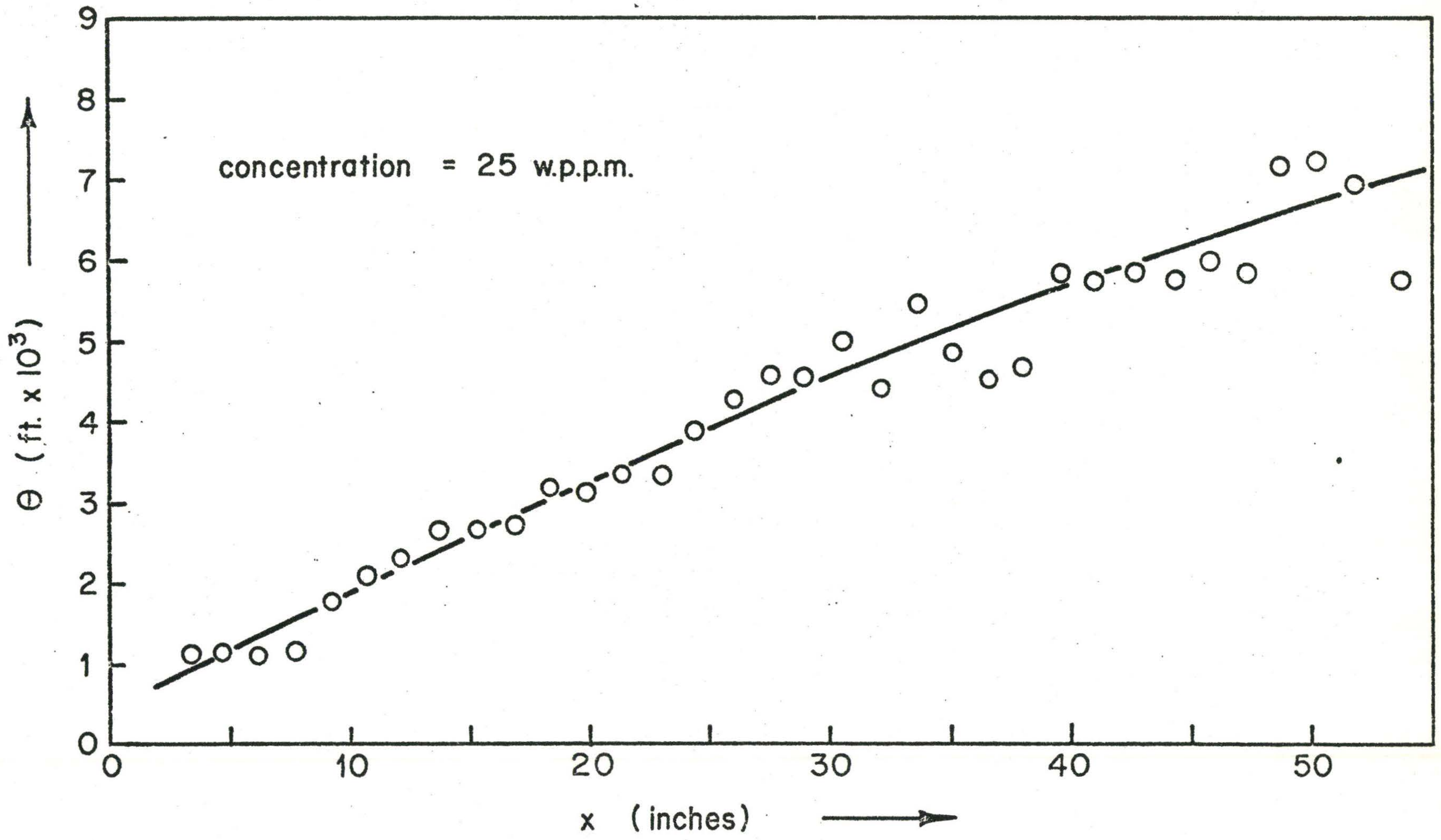

MOMENTUM THICKNESS vs X

FIGURE 12

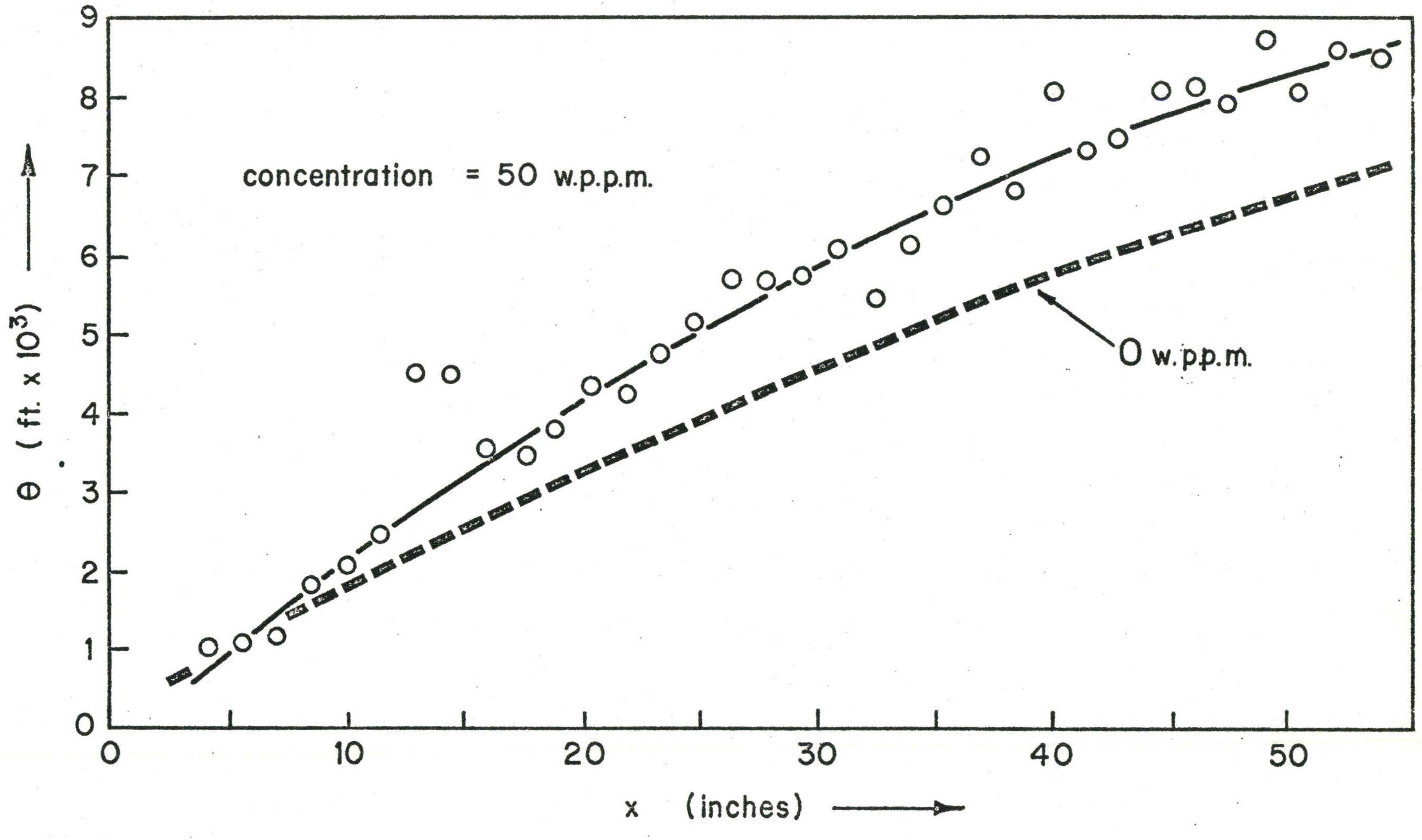

MOMENTUM THICKNESS vs X

FIGURE 13

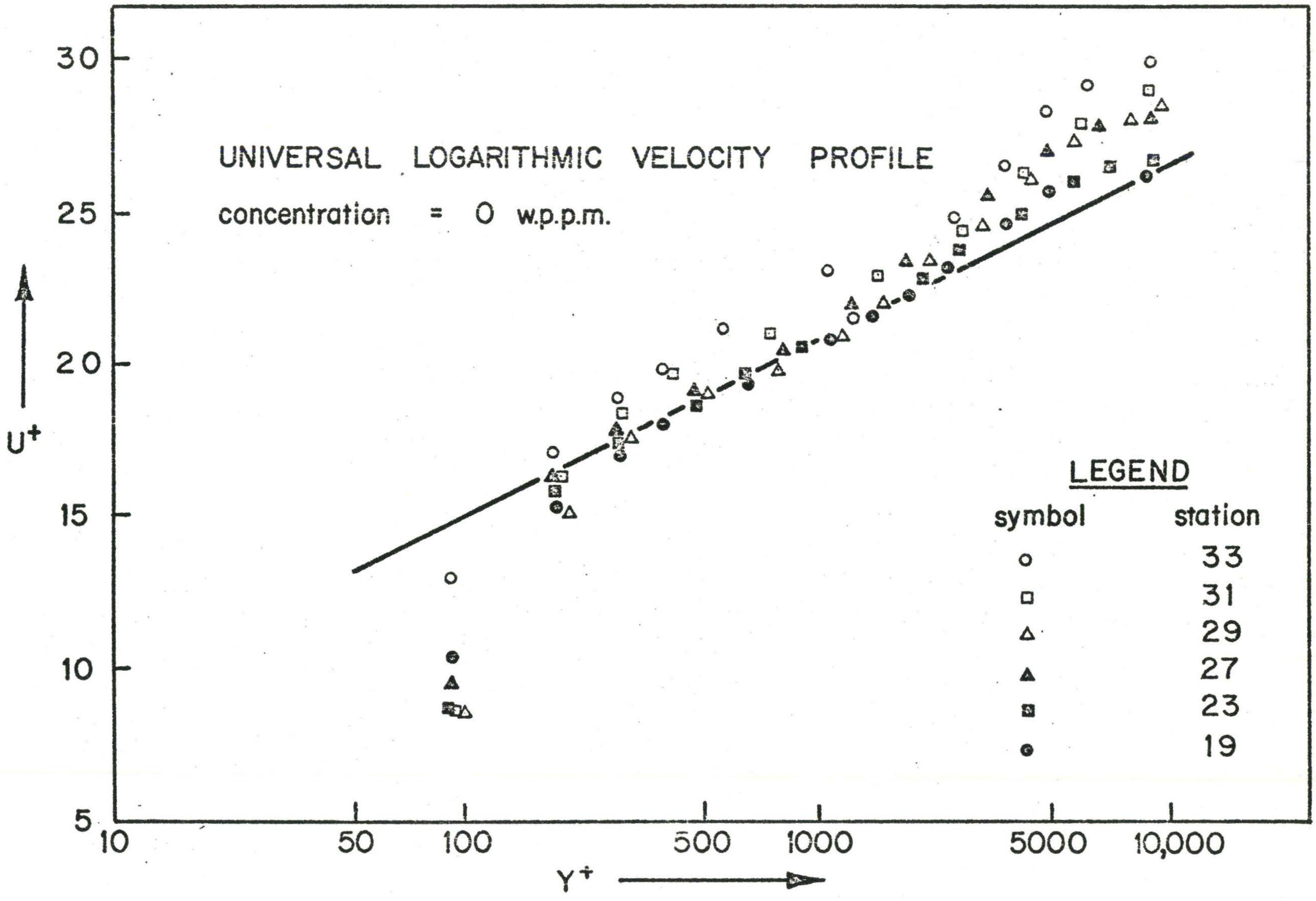

Y^+ vs U^+

FIGURE 14

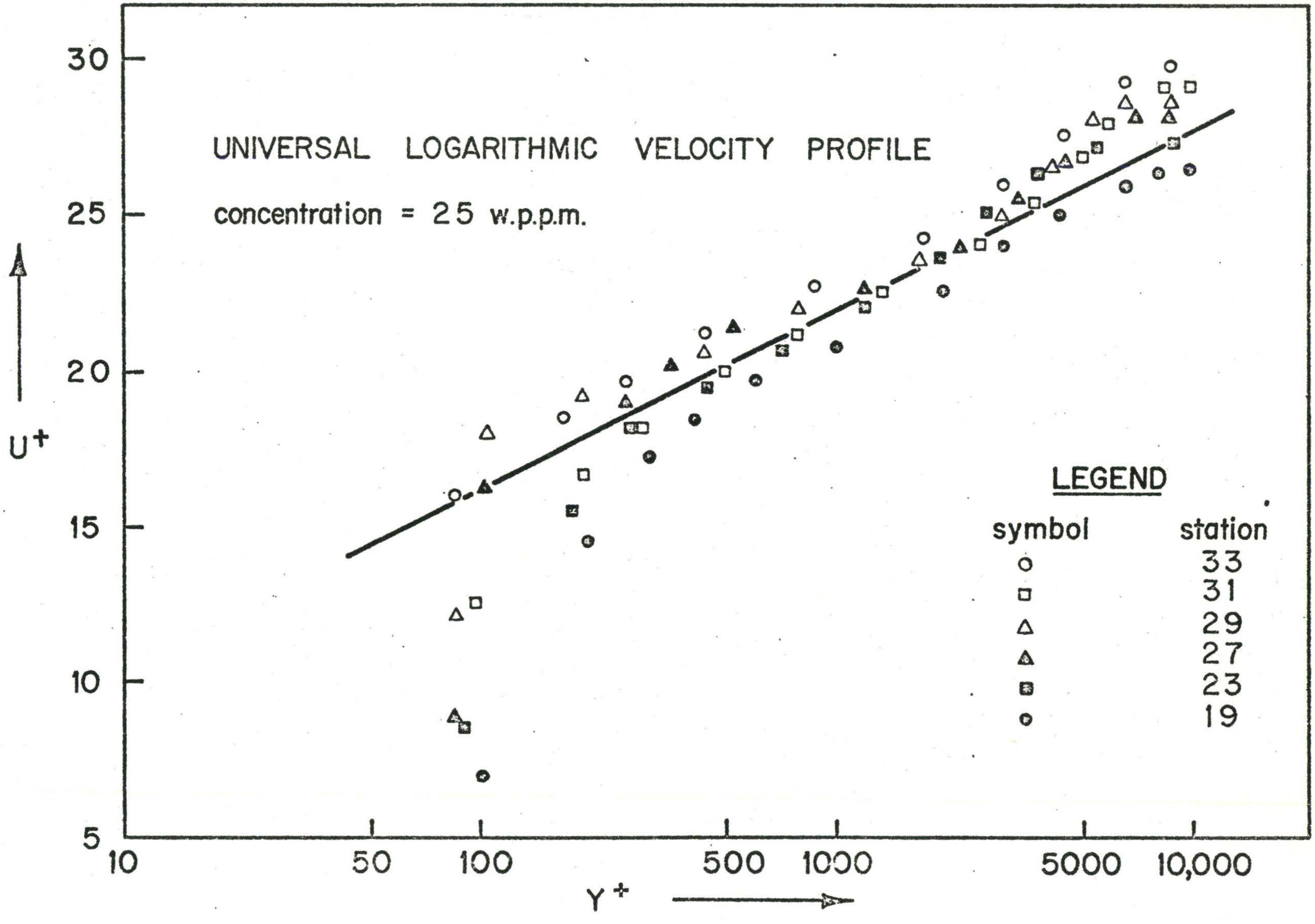

Y^+ vs U^+

FIGURE 15

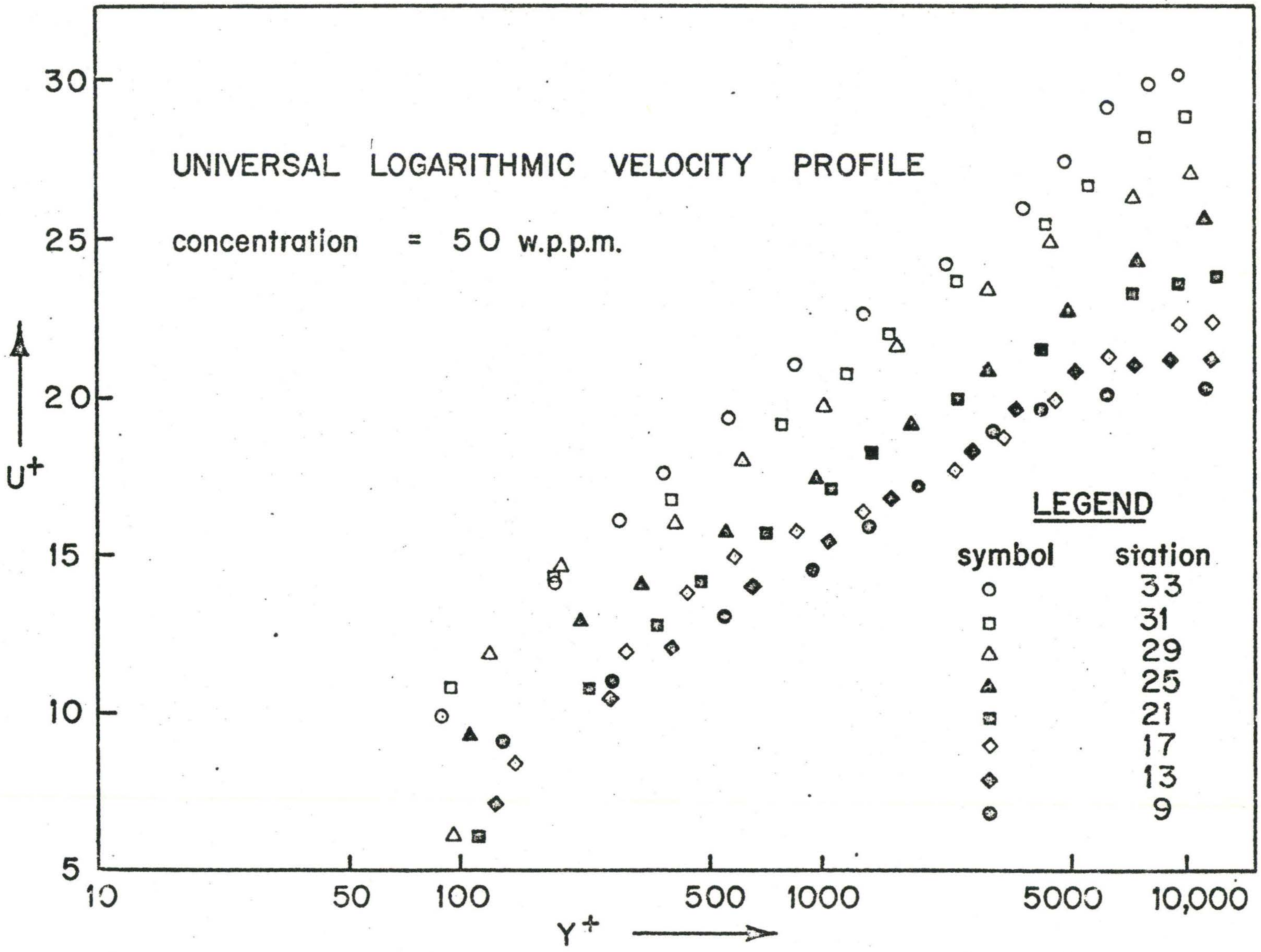

U+ vs Y+

FIGURE 16

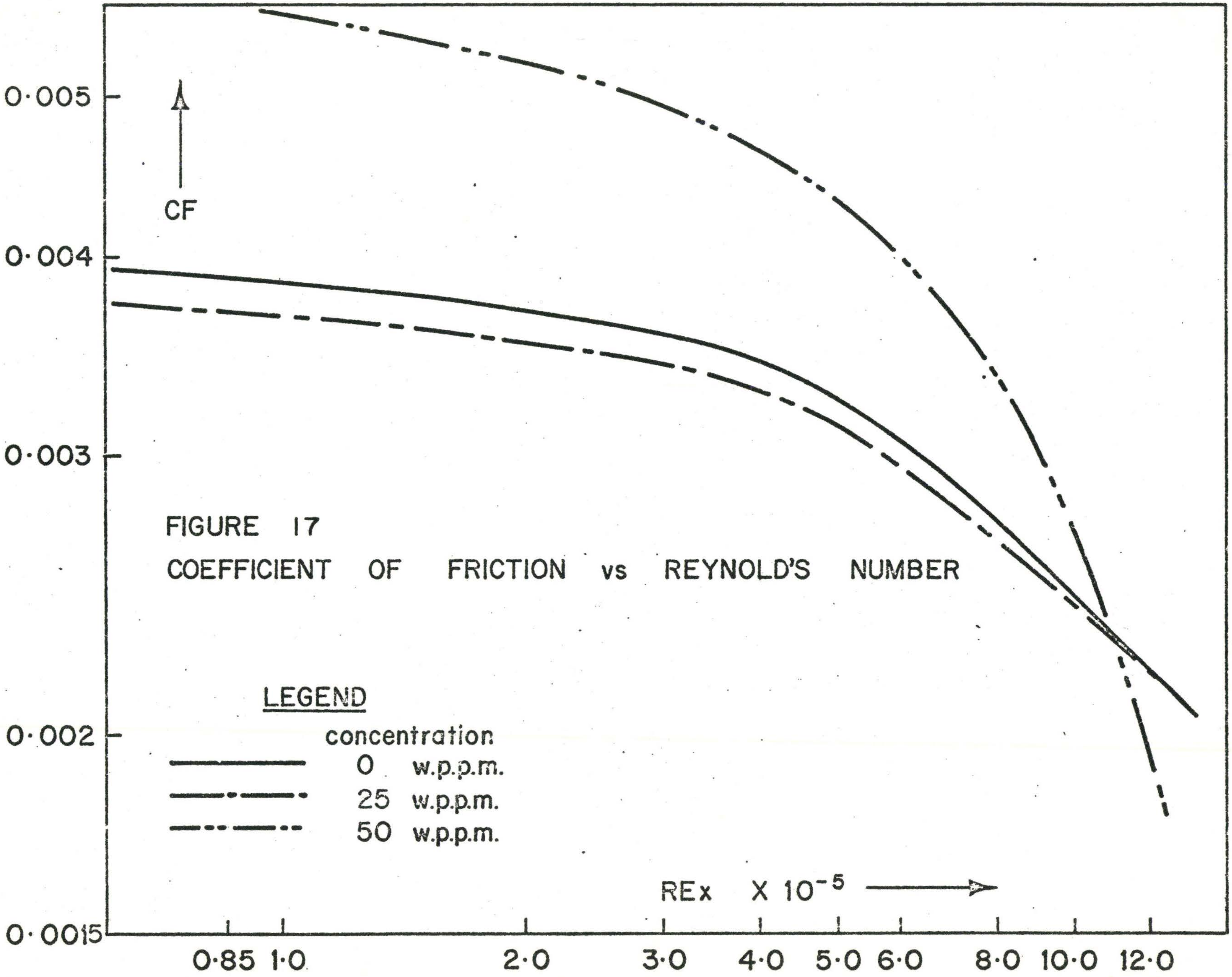

FIGURE 17
COEFFICIENT OF FRICTION vs REYNOLD'S NUMBER

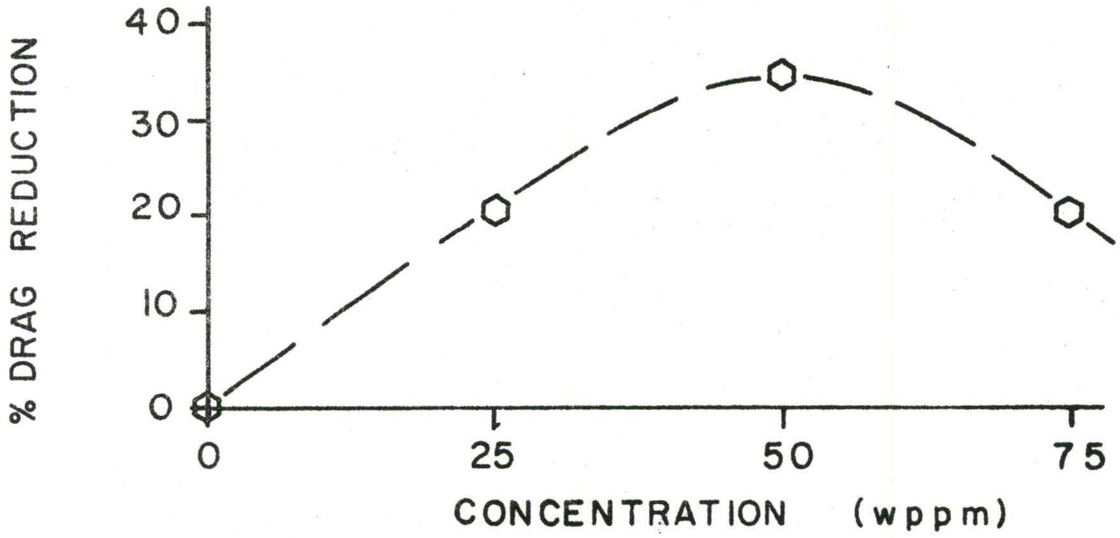

% DRAG REDUCTION vs CONCENTRATION

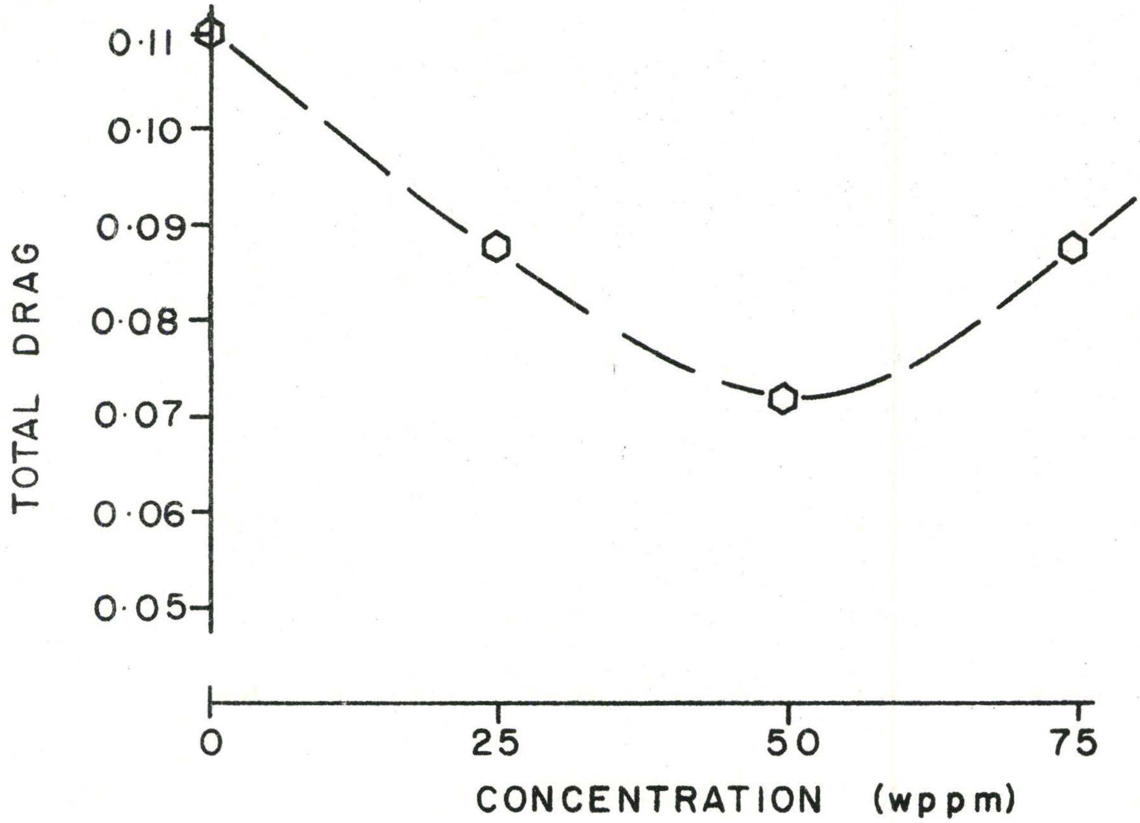

DRAG vs CONCENTRATION

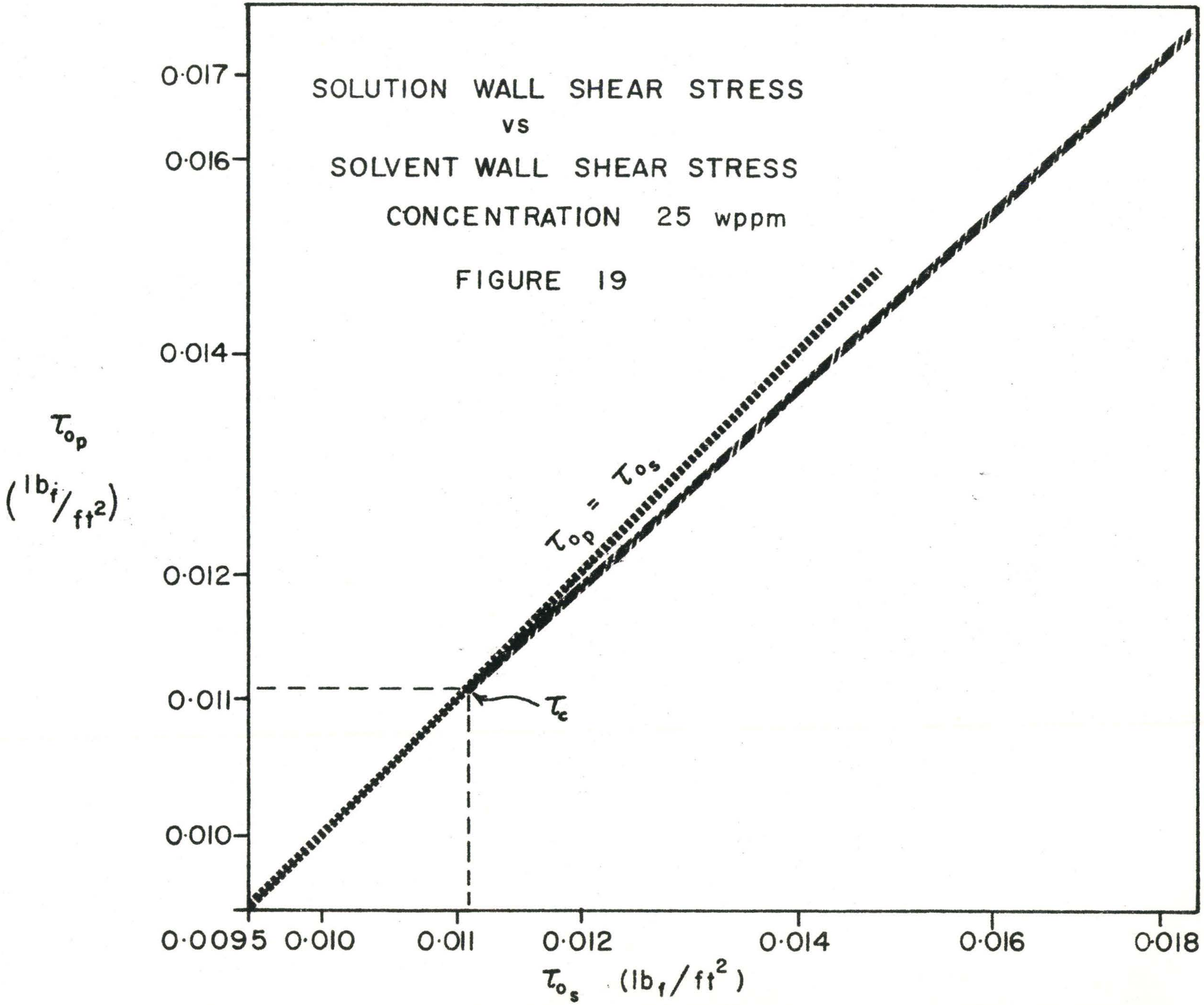
SOLUTION WALL SHEAR STRESS
vs
SOLVENT WALL SHEAR STRESS
CONCENTRATION 25 wppm
FIGURE 19
$\tau_{op} = \tau_{os}$
τ_c
τ_{op}
(lb_f/ft^2)
0.017
0.016
0.014
0.012
0.011
0.010
0.0095
0.010
0.011
0.012
0.014
0.016
0.018
τ_{os} (lb_f/ft^2)

APPENDIX 1

Error Analysis

The error analysis shown here does not attempt to show the magnitude of all the errors but attempts to indicate the relative significance of each of the errors. This is because the calculations involved tend to be statistical in nature and the errors are difficult to evaluate.

1. Calibration of Hot-film Probes.

Using the pitot probe at a velocity of about 2'/sec, the manometer reading is about 2.0 ± 0.001 cm difference, and the anemometer output is about 17.40 ± 0.05 volts, then, since the velocity varies as the square root of the manometer reading, that is

$$(v = (2gh)^{1/2})$$

the per cent error in velocity is $\frac{1}{2}\left(\frac{.001}{2.00}\right) \times 100\% = 0.025\%$.

Using the neutrally bouyant particle calibration method for low velocities, at 1 foot per second $(V = \frac{\Delta x}{\Delta t})$

Δx is about $18 \pm 1/12$ ft.

Δt is about 18 ± 0.1 second.

The percentage error in velocity is then 1%.

The anemometer voltage reading at a fluid velocity of about 2.2 feet per second was about 18.0 ± 0.05 volts. The largest error would be encountered at higher velocities, since the velocity varies most rapidly with voltage in this range of the calibration curve. Taking into account the error in the calibration curve, the maximum error that would be experienced in the velocity is 1.5%.

2. Momentum Thickness.

From the above analysis it can be seen that the maximum error in calculating $\frac{u}{U_1}$ is about 3%. Because of the way the momentum thickness varies with position along the plate it is difficult to give one analysis which satisfies all profiles. It is felt that the maximum error in evaluating the momentum thickness is of the order of 0.001 inches. In fitting a least squares curve through the data the error in the resulting curve is estimated to be reduced to 0.0001 inches which would represent a maximum error of about 10% for low values of x and about 2% for large values of x.

3. Skin Friction and Drag Reduction.

It is assumed that the error in any parameter deduced from the momentum thickness profile will have an error approximately the same as the error in the momentum thickness. That is, the uncertainty in the local skin friction coefficient will be about 10% for low values of x and 2% for high values of x as will be the case for the friction velocity.

The evaluation of the uncertainty in the calculated total drag is difficult to evaluate since it will involve a statistical formulation.

The error in the directly measured drag consists of the uncertainty in the calibration of the displacement transducer and the error in the instrument reading. This uncertainty is of the order of 1%.

4. Universal Logarithmic Velocity Profile.

The errors in the parameters for this plot are dependent on the errors discussed so far. Since most of the profiles plotted are for large values of x uncertainties due to errors in the momentum thickness will be of the order of 2%.

Then the maximum uncertainty in the parameter U^* will be 6% while the uncertainty in Y^+ will be of the order of 3%.

APPENDIX II

Statistical Analysis of Results

This analysis is based on the difference between the various data points for the momentum thickness and the best fit curve for the pure water data. That is, the results roe pure water are taken as the parent family to which comparisons are made.

For the data for pure water the average weighted residual is 5×10^{-10} feet with a standard deviation of 0.000373 feet.

Since the best fit curves for the momentum thickness for pure water and hte 25 wppm solution cross near mid-way along the plate, the data were analysed in two sections.

For the first section of the curve, the average of the residuals of the data for the 25 wppm solution is 0.000103 feet. making the hypothesis that the data for the 25 wppm solution is the same as for pure water and applying Student's "t" test, the value t = 1.139 is obtained. For this value of t and 17 degrees of freedom, it is found that there is a 15% probability that the difference between the data could be due to chance which is generally taken to mean that the data are not statistically significantly different.

For the second section of the curve, a value of t = 1.59 is obtained, which for 14 degrees of freedom yields a 10% probability level which is considered not greatly significant.

Performing the same calculations for all the 50 wppm solution data, the average residual is 0.00108 feet and the value of t is 15.6. This value of t corresponds to a significance level much smaller than 0.1% which is interpreted as being highly significant.

APPENDIX III

Moisture Content of Polymer Sample

The polymer used was a Stein-Hall polyacrylamide, Polyhall 402. The method used is as outlined in Chapter IV-2.

Weight of dry crucible	28.56195 gm.
Weight of crucible plus moist sample	37.13810 gm.
Weight of crucible plus dried sample	36.85420 gm.
Moisture content	0.28390 gm.
Weight of dried polymer	8.29225 gm.
Per cent moisture in sample	3.313 %

APPENDIX IV

Calibration Curves

Calibration curves for the hot-film probes used are shown in Figure (20). The overheating ratio for the cylindrical probe was 0.0057. For the conical probe the overheating ratio was 0.100.

The calibration for the drag measuring system is shown in Figure (21).

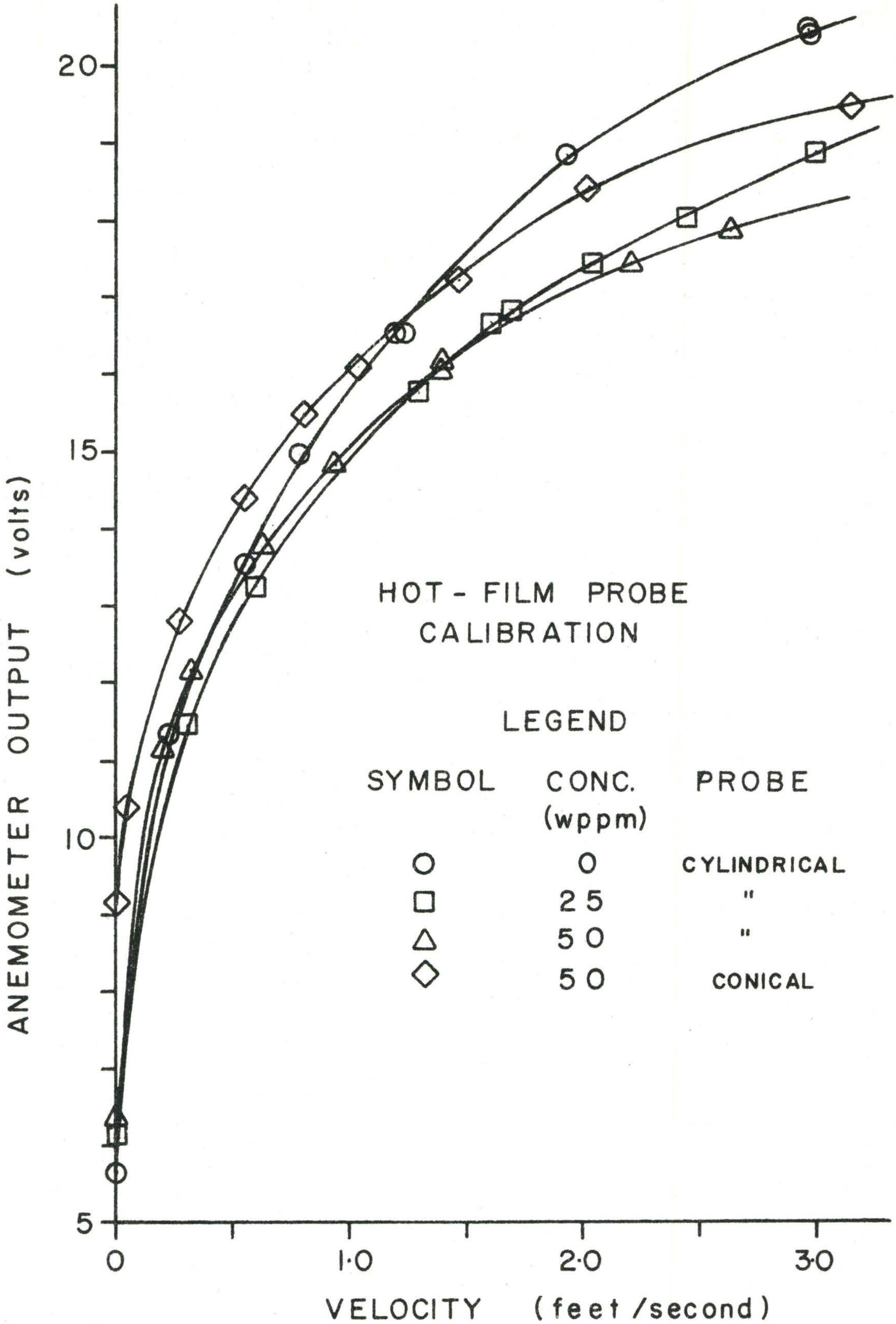
20
15
10
5
ANEMOMETER OUTPUT (volts)
0
1·0
2·0
3·0
VELOCITY (feet /second)
HOT - FILM PROBE
CALIBRATION
LEGEND
SYMBOL
CONC. (wppm)
PROBE
0
CYLINDRICAL
25
"
50
"
50
CONICAL

FIGURE 20

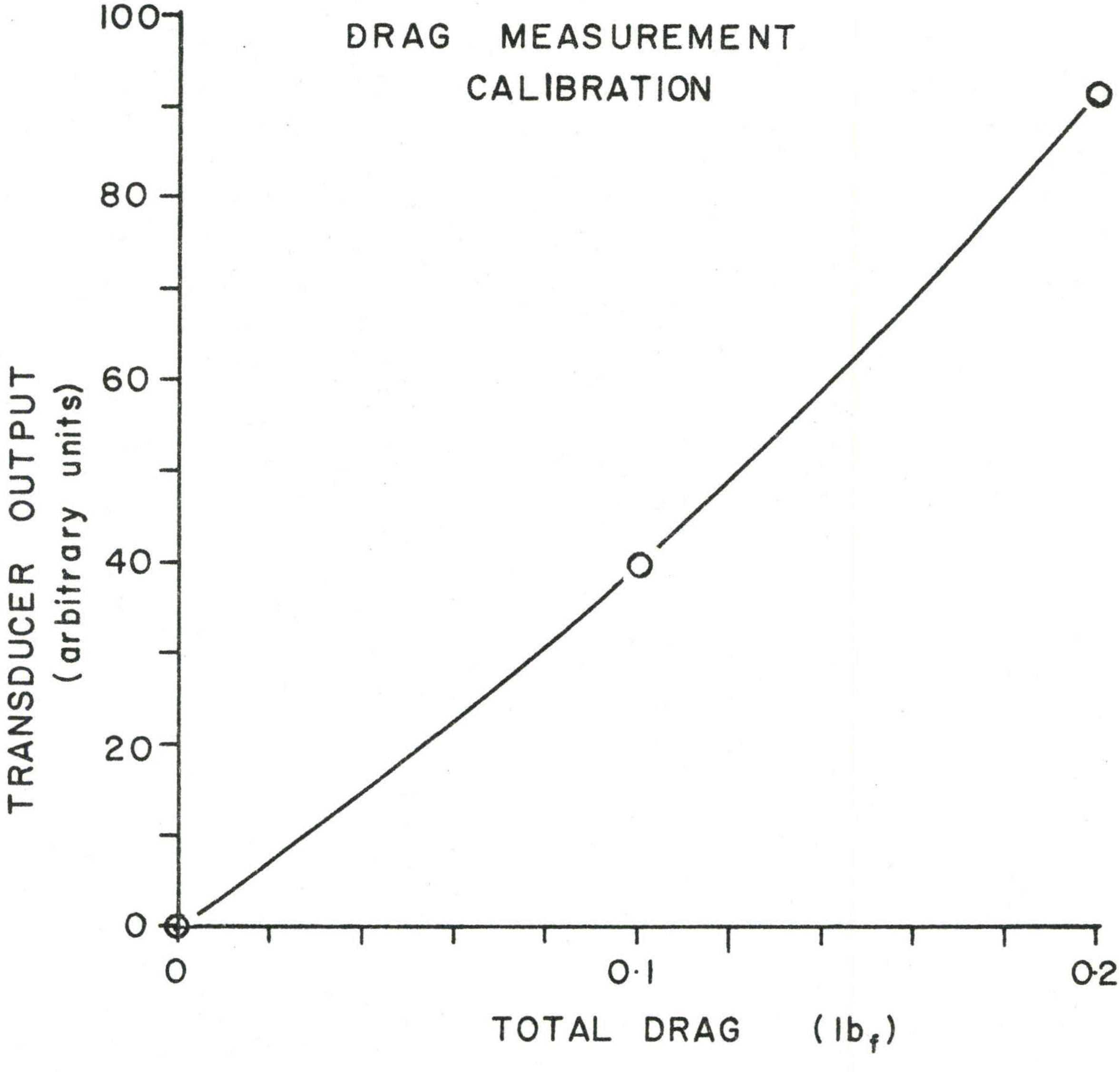
DRAG MEASUREMENT
CALIBRATION
TRANSDUCER OUTPUT
(arbitrary units)
100
80
60
40
20
0
0
0·1
0·2
TOTAL DRAG (lb$_f$)

FIGURE 21

APPENDIX V

Data Tables

The experimental data for the three concentrations, 0, 25 and 50 wppm are shown in Tables 1, 2 and 3 respectively.

In each table the upper three numbers are the coefficients of the polynomial, $\theta = X1x^2 + X2x + X3$. The number on the second line represents the number of velocity profiles for the particular concentration. For each profile the first quantity is the corresponding value for x, the second is the calculated momentum thickness and the third is the velocity at the edge of the outer boundary layer. The subsequent 35 numbers (left to right) represent the magnitudes of the velocity ratios u/U_1 for the values of y generated by the computer program.

Tables 4, 5 and 6 show the values of the derived parameters for the concentrations 0, 25 and 50 wppm respectively. The first column of numbers is the station number along the plate which appears in Figures (8, 9, 10, 14, 15, 16).

```
-7.07054E-07   1.664856E-04   1.51785E-04
35
        3.342       3.8313E-04         2.221
0.676 0.839 0.931 0.969 0.989 0.999 0.999 0.999 0.999 0.999 0.999 0.999 0.999
0.999 0.999 0.999 0.999 0.999 0.999 0.999 0.999 0.999 0.999 0.999 0.999 0.999
0.999 0.999 0.999 0.999 0.999 0.999 0.999 0.999 0.999
        4.243       7.3021E-04         2.205
0.519 0.706 0.804 0.881 0.929 0.957 0.974 0.985 0.991 0.999 0.998 0.999 0.999
0.999 0.999 0.999 0.999 0.999 0.999 0.999 0.999 0.999 0.999 0.999 0.999 0.999
0.999 0.999 0.999 0.999 0.999 0.999 0.999 0.999 0.999
        5.440       7.2988E-04         2.221
0.604 0.768 0.847 0.890 0.919 0.945 0.959 0.973 0.981 0.991 0.997 0.999 0.999
0.999 0.999 0.999 0.999 0.999 0.999 0.999 0.999 0.999 0.999 0.999 0.999 0.999
0.999 0.999 0.999 0.999 0.999 0.999 0.999 0.999 0.999
        6.475       2.1006E-03         2.221
0.381 0.596 0.652 0.691 0.721 0.746 0.768 0.787 0.804 0.823 0.873 0.925 0.945
0.987 0.999 0.999 0.999 0.999 0.999 0.999 0.999 0.999 0.999 0.999 0.999 0.999
0.999 0.999 0.999 0.999 0.999 0.999 0.999 0.999 0.999
        7.701       1.7813E-03         2.320
0.430 0.689 0.768 0.807 0.834 0.855 0.869 0.881 0.893 0.902 0.915 0.927 0.941
0.953 0.967 0.978 0.987 0.995 0.999 0.999 0.999 0.999 0.999 0.999 0.999 0.999
0.999 0.999 0.999 0.999 0.999 0.999 0.999 0.999 0.999
        9.180       2.1969E-03         2.215
0.559 0.673 0.731 0.770 0.807 0.831 0.854 0.870 0.882 0.893 0.912 0.922 0.935
0.940 0.946 0.955 0.961 0.967 0.973 0.980 0.991 0.999 0.999 0.999 0.999 0.999
0.999 0.999 0.999 0.999 0.999 0.999 0.999 0.999 0.999
       10.466       2.3516E-03         2.221
0.487 0.707 0.785 0.825 0.855 0.875 0.893 0.904 0.913 0.917 0.927 0.935 0.940
0.949 0.951 0.953 0.955 0.958 0.962 0.964 0.968 0.974 0.980 0.985 0.990 0.995
0.997 0.999 0.999 0.999 0.999 0.999 0.999 0.999 0.999
       12.052       2.0674E-03         2.221
0.465 0.661 0.729 0.767 0.793 0.813 0.831 0.847 0.861 0.875 0.897 0.915 0.931
0.945 0.958 0.971 0.983 0.991 0.999 0.999 0.999 0.999 0.999 0.998 0.999 0.999
0.999 0.999 0.999 0.999 0.999 0.999 0.999 0.999 0.999
```

TABLE 1

DATA FOR CONCENTRATION 0 wppm

	13.565		2.5391E-03			2.221						
0.500	0.643	0.706	0.741	0.769	0.793	0.817	0.833	0.849	0.865	0.890	0.910	0.921
0.938	0.947	0.955	0.961	0.967	0.971	0.977	0.982	0.988	0.992	0.997	0.999	0.999
0.999	0.999	0.999	0.999	0.999	0.999	0.999	0.999	0.999				
	15.108		2.3002E-03			2.221						
0.474	0.677	0.738	0.769	0.791	0.811	0.829	0.841	0.857	0.868	0.891	0.909	0.924
0.939	0.951	0.962	0.970	0.978	0.983	0.988	0.994	0.997	0.992	0.997	0.999	0.999
0.999	0.999	0.999	0.999	0.999	0.999	0.999	0.999	0.999				
	16.556		4.7852E-03			2.221						
0.377	0.587	0.641	0.675	0.704	0.727	0.747	0.769	0.786	0.795	0.815	0.831	0.849
0.862	0.869	0.876	0.884	0.890	0.898	0.904	0.917	0.931	0.939	0.953	0.967	0.979
0.991	0.999	0.999	0.999	0.999	0.999	0.999	0.999	0.999				
	18.046		3.0979E-03			2.275						
0.256	0.407	0.480	0.556	0.612	0.655	0.701	0.733	0.764	0.791	0.837	0.877	0.908
0.931	0.947	0.959	0.965	0.971	0.974	0.977	0.980	0.982	0.985	0.990	0.994	0.998
0.999	0.999	0.999	0.999	0.999	0.999	0.999	0.999	0.999				
	19.608		3.5967E-03			2.645						
0.389	0.605	0.680	0.705	0.723	0.751	0.775	0.787	0.797	0.807	0.833	0.856	0.875
0.891	0.905	0.919	0.925	0.937	0.942	0.951	0.959	0.968	0.975	0.985	0.990	0.995
0.997	0.999	0.999	0.999	0.999	0.999	0.999	0.999	0.999				
	20.995		3.2802E-03			2.680						
0.369	0.606	0.685	0.727	0.759	0.782	0.799	0.811	0.821	0.831	0.849	0.865	0.880
0.895	0.907	0.917	0.925	0.937	0.945	0.953	0.967	0.977	0.985	0.993	0.997	0.999
0.999	0.998	0.999	0.999	0.999	0.999	0.999	0.999	0.999				
	22.400		3.7097E-03			2.750						
0.367	0.601	0.677	0.717	0.740	0.751	0.765	0.775	0.785	0.795	0.812	0.833	0.851
0.867	0.883	0.897	0.913	0.927	0.937	0.947	0.962	0.973	0.983	0.991	0.996	0.997
0.999	0.999	0.999	0.999	0.999	0.999	0.999	0.999	0.999				
	23.952		3.6707E-03			2.675						
0.269	0.558	0.643	0.693	0.719	0.733	0.749	0.760	0.770	0.787	0.806	0.825	0.842
0.863	0.880	0.896	0.909	0.922	0.935	0.947	0.965	0.981	0.995	0.998	0.999	0.999
0.999	0.999	0.999	0.999	0.999	0.999	0.999	0.999	0.999				
	25.553		4.2699E-03			2.670						
0.329	0.573	0.657	0.707	0.733	0.751	0.763	0.773	0.783	0.793	0.811	0.829	0.839
0.857	0.869	0.881	0.891	0.903	0.913	0.923	0.939	0.955	0.968	0.977	0.983	0.990
0.991	0.999	0.999	0.999	0.999	0.999	0.999	0.999	0.999				

Table 1 continued

	27.950		3.5998E-03			2.445						
0.463	0.641	0.665	0.690	0.706	0.721	0.737	0.754	0.768	0.785	0.809	0.837	0.857
0.871	0.887	0.903	0.917	0.930	0.941	0.953	0.971	0.983	0.991	0.997	0.999	0.998
0.999	0.998	0.999	0.999	0.999	0.999	0.999	0.999	0.999				
	29.065		4.2290E-03			2.335						
0.405	0.606	0.659	0.700	0.719	0.729	0.747	0.763	0.781	0.797	0.807	0.821	0.835
0.849	0.865	0.877	0.889	0.898	0.911	0.917	0.936	0.955	0.969	0.984	0.995	0.999
0.999	0.999	0.999	0.999	0.999	0.999	0.999	0.999	0.999				
	30.348		4.1293E-03			2.430						
0.407	0.625	0.681	0.716	0.741	0.761	0.779	0.793	0.806	0.819	0.843	0.861	0.879
0.893	0.903	0.917	0.923	0.931	0.937	0.943	0.953	0.957	0.962	0.967	0.971	0.975
0.981	0.987	0.989	0.993	0.993	0.996	0.997	0.999	0.999				
	31.941		4.5465E-03			2.365						
0.363	0.619	0.689	0.719	0.738	0.759	0.774	0.789	0.799	0.811	0.829	0.845	0.859
0.873	0.883	0.894	0.903	0.910	0.917	0.923	0.933	0.943	0.951	0.957	0.965	0.973
0.982	0.991	0.991	0.997	0.997	0.997	0.997	0.997	0.999				
	33.455		4.8910E-03			2.365						
0.362	0.621	0.679	0.713	0.729	0.743	0.759	0.769	0.777	0.785	0.801	0.819	0.833
0.844	0.856	0.869	0.879	0.891	0.901	0.911	0.923	0.937	0.951	0.961	0.971	0.975
0.982	0.989	0.993	0.997	0.997	0.997	0.997	0.999	0.999				
	35.015		5.5430E-03			2.405						
0.323	0.591	0.643	0.677	0.699	0.715	0.733	0.749	0.759	0.773	0.789	0.805	0.819
0.832	0.844	0.855	0.867	0.878	0.887	0.897	0.911	0.922	0.933	0.945	0.956	0.966
0.975	0.985	0.987	0.991	0.993	0.994	0.994	0.997	0.998				
	38.000		5.8284E-03			2.420						
0.398	0.599	0.666	0.703	0.723	0.737	0.744	0.753	0.761	0.767	0.781	0.797	0.807
0.821	0.833	0.841	0.853	0.867	0.877	0.884	0.905	0.921	0.937	0.949	0.957	0.967
0.977	0.980	0.983	0.983	0.984	0.985	0.990	0.992	0.995				
	39.532		5.0250E-03			2.375						
0.393	0.661	0.694	0.706	0.717	0.728	0.739	0.748	0.755	0.767	0.789	0.803	0.819
0.837	0.851	0.857	0.867	0.877	0.888	0.896	0.911	0.929	0.941	0.957	0.968	0.983
0.992	0.997	0.997	0.999	0.999	0.999	0.999	0.999	0.999				
	41.068		4.7126E-03			2.490						
0.447	0.586	0.641	0.691	0.711	0.728	0.740	0.759	0.770	0.791	0.809	0.824	0.837
0.850	0.861	0.872	0.881	0.891	0.900	0.919	0.931	0.945	0.953	0.961	0.972	0.980
0.989	0.993	0.997	0.999	0.999	0.999	0.999	0.999	0.999				

Table 1 continued

	42.553		5.5237E-03			2.500						
0.338	0.583	0.636	0.663	0.683	0.698	0.711	0.721	0.730	0.741	0.762	0.761	0.799
0.818	0.833	0.849	0.861	0.873	0.883	0.892	0.911	0.928	0.942	0.953	0.961	0.972
0.980	0.985	0.990	0.993	0.996	0.999	0.999	0.999	0.999				
	44.105		6.1730E-03			2.785						
0.282	0.533	0.621	0.667	0.693	0.711	0.723	0.734	0.745	0.755	0.771	0.787	0.800
0.815	0.831	0.843	0.857	0.869	0.883	0.891	0.913	0.929	0.941	0.949	0.952	0.955
0.959	0.964	0.969	0.973	0.976	0.983	0.987	0.991	0.995				
	45.608		6.8502E-03			2.765						
0.303	0.527	0.615	0.645	0.664	0.677	0.687	0.696	0.704	0.711	0.730	0.749	0.771
0.789	0.809	0.819	0.830	0.841	0.851	0.860	0.879	0.895	0.910	0.926	0.940	0.957
0.969	0.971	0.973	0.976	0.979	0.985	0.989	0.992	0.996				
	47.125		6.6670E-03			2.670						
0.399	0.543	0.609	0.639	0.653	0.667	0.681	0.693	0.700	0.712	0.731	0.750	0.765
0.781	0.797	0.809	0.823	0.835	0.845	0.855	0.875	0.890	0.907	0.921	0.931	0.945
0.963	0.977	0.991	0.999	0.999	0.999	0.999	0.999	0.999				
	48.638		7.0063E-03			2.690						
0.296	0.559	0.629	0.667	0.687	0.699	0.713	0.722	0.732	0.743	0.757	0.771	0.783
0.793	0.801	0.810	0.817	0.826	0.837	0.845	0.864	0.885	0.902	0.913	0.925	0.941
0.955	0.964	0.976	0.987	0.987	0.991	0.991	0.991	0.996				
	50.611		6.4710E-03			2.690						
0.411	0.541	0.598	0.629	0.659	0.685	0.715	0.727	0.733	0.741	0.753	0.767	0.775
0.783	0.791	0.799	0.809	0.817	0.825	0.839	0.855	0.879	0.902	0.925	0.947	0.967
0.981	0.989	0.997	0.999	0.999	0.999	0.999	0.999	0.999				
	52.736		7.3246E-03			2.690						
0.429	0.567	0.625	0.661	0.687	0.705	0.720	0.731	0.743	0.755	0.767	0.779	0.786
0.793	0.799	0.801	0.807	0.811	0.819	0.828	0.848	0.878	0.901	0.923	0.939	0.948
0.959	0.965	0.969	0.971	0.973	0.975	0.977	0.985	0.993				
	54.538		6.6457E-03			2.705						
0.473	0.623	0.665	0.698	0.720	0.731	0.743	0.755	0.761	0.765	0.774	0.785	0.793
0.799	0.812	0.819	0.831	0.841	0.849	0.859	0.871	0.887	0.897	0.913	0.929	0.945
0.957	0.970	0.981	0.986	0.993	0.996	0.995	0.995	0.995				
	55.721		4.7130E-03			2.625						
0.528	0.653	0.703	0.740	0.763	0.784	0.801	0.817	0.831	0.839	0.857	0.871	0.879
0.885	0.893	0.899	0.905	0.909	0.911	0.917	0.927	0.933	0.943	0.952	0.957	0.965
0.971	0.973	0.983	0.993	0.993	0.994	0.995	0.995	0.995				

Table 1 continued

-6.06697E-07 1.57164E-04 3.4389E-04

35

3.379	1.0560E-03	2.540										
0.518	0.784	0.834	0.870	0.899	0.918	0.931	0.940	0.949	0.958	0.970	0.979	0.984
0.988	0.989	0.995	0.997	0.998	0.998	0.999	0.999	0.999	0.999	0.999	0.999	0.999
0.999	0.998	0.999	0.999	0.998	0.999	0.998	0.999	0.999				
4.859	1.1221E-03	2.625										
0.443	0.760	0.829	0.869	0.898	0.916	0.927	0.939	0.948	0.957	0.965	0.973	0.979
0.987	0.989	0.990	0.991	0.995	0.999	0.999	0.999	0.999	0.999	0.999	0.999	0.999
0.998	0.998	0.998	0.998	0.998	0.998	0.998	0.998	0.999				
6.354	1.1030E-03	2.385										
0.605	0.733	0.795	0.838	0.866	0.889	0.911	0.927	0.940	0.953	0.974	0.985	0.993
0.996	0.999	0.999	0.999	0.999	0.999	0.999	0.999	0.998	0.998	0.998	0.999	0.998
0.999	0.998	0.998	0.999	0.999	0.999	0.999	0.998	0.999				
7.811	1.1286E-03	2.455										
0.446	0.672	0.762	0.818	0.863	0.890	0.911	0.929	0.944	0.959	0.976	0.991	0.994
0.998	0.999	0.998	0.999	0.999	0.999	0.999	0.999	0.999	0.999	0.999	0.999	0.999
0.999	0.999	0.999	0.999	0.999	0.999	0.999	0.999	0.999				
9.354	1.7295E-03	2.455										
0.469	0.649	0.725	0.769	0.801	0.828	0.851	0.872	0.889	0.901	0.923	0.943	0.959
0.971	0.983	0.991	0.994	0.999	0.999	0.999	0.999	0.999	0.999	0.998	0.999	0.999
0.998	0.998	0.998	0.999	0.998	0.999	0.999	0.999	0.998				
10.793	2.0800E-03	2.500										
0.301	0.601	0.703	0.754	0.790	0.808	0.825	0.845	0.855	0.869	0.895	0.918	0.935
0.949	0.961	0.973	0.981	0.991	0.995	0.997	0.999	0.999	0.999	0.998	0.999	0.999
0.998	0.998	0.998	0.998	0.998	0.998	0.998	0.999	0.998				
12.321	2.2822E-03	2.360										
0.567	0.713	0.767	0.799	0.815	0.833	0.851	0.863	0.875	0.884	0.899	0.913	0.923
0.937	0.945	0.955	0.963	0.971	0.977	0.979	0.986	0.991	0.996	0.998	0.998	0.999
0.999	0.998	0.999	0.999	0.999	0.999	0.999	0.999	0.999				
13.880	2.6106E-03	2.355										
0.391	0.621	0.708	0.750	0.784	0.810	0.831	0.848	0.863	0.878	0.889	0.915	0.929
0.936	0.941	0.949	0.958	0.964	0.968	0.970	0.978	0.981	0.986	0.991	0.996	0.998
0.999	0.999	0.999	0.999	0.999	0.999	0.999	0.999	0.999				

TABLE 2

DATA FOR CONCENTRATION 25 wppm

	15.402		2.6606E-03			2.300						
0.471	0.693	0.757	0.797	0.829	0.847	0.861	0.875	0.883	0.891	0.903	0.915	0.923
0.931	0.935	0.939	0.947	0.951	0.954	0.960	0.971	0.973	0.979	0.985	0.991	0.999
0.995	0.995	0.997	0.999	0.999	0.998	0.999	0.999	0.999				
	17.020		2.6897E-03			2.335						
0.383	0.639	0.715	0.758	0.793	0.807	0.821	0.837	0.848	0.857	0.874	0.888	0.899
0.914	0.923	0.933	0.944	0.953	0.963	0.971	0.989	0.993	0.998	0.999	0.999	0.997
0.998	0.995	0.999	0.999	0.999	0.999	0.999	0.998	0.997				
	18.528		3.1263E-03			2.625						
0.473	0.659	0.720	0.751	0.775	0.793	0.808	0.817	0.829	0.839	0.854	0.868	0.881
0.893	0.905	0.917	0.927	0.939	0.948	0.955	0.969	0.981	0.994	0.999	0.999	0.998
0.998	0.999	0.999	0.999	0.999	0.999	0.999	0.999	0.999				
	20.024		3.1164E-03			2.555						
0.503	0.663	0.702	0.733	0.757	0.775	0.793	0.804	0.815	0.826	0.847	0.865	0.883
0.899	0.913	0.926	0.935	0.943	0.954	0.960	0.974	0.985	0.991	0.998	0.999	0.999
0.999	0.997	0.999	0.999	0.999	0.999	0.999	0.999	0.999				
	21.536		3.3336E-03			2.600						
0.367	0.635	0.719	0.751	0.777	0.797	0.811	0.821	0.841	0.855	0.873	0.891	0.907
0.918	0.929	0.936	0.945	0.949	0.959	0.962	0.974	0.975	0.978	0.980	0.982	0.984
0.986	0.988	0.990	0.992	0.994	0.996	0.997	0.998	0.999				
	23.125		3.3120E-03			2.625						
0.509	0.655	0.709	0.739	0.765	0.785	0.800	0.812	0.825	0.837	0.852	0.867	0.877
0.887	0.899	0.912	0.921	0.934	0.940	0.949	0.964	0.975	0.989	0.995	0.998	0.998
0.999	0.999	0.999	0.999	0.999	0.999	0.999	0.999	0.999				
	24.552		3.8769E-03			2.625						
0.445	0.653	0.715	0.749	0.771	0.787	0.799	0.807	0.817	0.822	0.839	0.854	0.863
0.877	0.887	0.898	0.908	0.917	0.927	0.935	0.953	0.968	0.977	0.982	0.984	0.988
0.991	0.991	0.993	0.995	0.998	0.998	0.999	0.999	0.999				
	26.079		4.2637E-03			2.530						
0.429	0.609	0.679	0.717	0.745	0.764	0.783	0.797	0.807	0.822	0.837	0.851	0.861
0.873	0.879	0.889	0.897	0.901	0.909	0.918	0.929	0.942	0.956	0.965	0.977	0.985
0.996	0.999	0.999	0.999	0.999	0.999	0.999	0.999	0.999				
	27.598		4.5385E-03			2.530						
0.511	0.626	0.673	0.699	0.719	0.734	0.751	0.760	0.769	0.779	0.798	0.814	0.831
0.851	0.865	0.877	0.889	0.900	0.911	0.921	0.935	0.948	0.957	0.966	0.975	0.987
0.995	0.997	0.998	0.999	0.999	0.998	0.999	0.999	0.999				

Table 2 continued

	29.124		4.5151E-03			2.640						
0.501	0.595	0.641	0.679	0.703	0.725	0.743	0.758	0.773	0.787	0.802	0.819	0.830
0.843	0.849	0.861	0.873	0.885	0.897	0.907	0.929	0.948	0.965	0.979	0.989	0.996
0.999	0.999	0.999	0.999	0.999	0.999	0.999	0.999	0.999				
	30.630		4.9945E-03			2.600						
0.271	0.550	0.650	0.695	0.724	0.743	0.757	0.767	0.777	0.784	0.799	0.813	0.829
0.846	0.856	0.867	0.879	0.889	0.903	0.909	0.925	0.937	0.949	0.959	0.964	0.968
0.976	0.983	0.992	0.994	0.999	0.999	0.999	0.999	0.999				
	32.168		4.3765E-03			2.590						
0.409	0.579	0.650	0.689	0.711	0.731	0.746	0.763	0.771	0.784	0.805	0.824	0.849
0.869	0.886	0.901	0.913	0.921	0.929	0.937	0.943	0.951	0.959	0.961	0.971	0.979
0.987	0.995	0.998	0.999	0.999	0.999	0.999	0.999	0.999				
	33.664		5.4313E-03			2.595						
0.342	0.555	0.639	0.686	0.721	0.741	0.761	0.776	0.789	0.800	0.819	0.834	0.846
0.857	0.868	0.875	0.884	0.890	0.896	0.903	0.913	0.922	0.931	0.939	0.950	0.959
0.969	0.976	0.980	0.984	0.989	0.991	0.996	0.999	0.999				
	35.136		4.8145E-03			2.375						
0.524	0.649	0.695	0.722	0.744	0.762	0.773	0.787	0.795	0.802	0.817	0.828	0.838
0.851	0.859	0.872	0.883	0.889	0.899	0.909	0.923	0.939	0.952	0.961	0.969	0.977
0.983	0.989	0.991	0.993	0.995	0.995	0.999	0.999	0.999				
	36.664		4.4692E-03			2.380						
0.316	0.570	0.661	0.691	0.714	0.730	0.744	0.757	0.768	0.778	0.795	0.811	0.826
0.840	0.855	0.869	0.881	0.894	0.909	0.919	0.939	0.954	0.969	0.976	0.981	0.988
0.993	0.999	0.999	0.999	0.999	0.999	0.999	0.999	0.999				
	38.232		4.6571E-03			2.320						
0.335	0.604	0.674	0.710	0.734	0.753	0.768	0.779	0.790	0.800	0.816	0.830	0.843
0.854	0.865	0.876	0.887	0.896	0.906	0.916	0.931	0.949	0.959	0.966	0.970	0.979
0.987	0.990	0.991	0.993	0.994	0.996	0.998	0.999	0.999				
	39.728		5.8333E-03			2.370						
0.335	0.566	0.629	0.649	0.671	0.688	0.700	0.712	0.722	0.732	0.751	0.768	0.781
0.797	0.812	0.829	0.839	0.853	0.866	0.879	0.899	0.920	0.939	0.949	0.960	0.971
0.980	0.987	0.992	0.995	0.996	0.997	0.998	0.999	0.999				
	41.259		5.7489E-03			2.385						
0.340	0.615	0.677	0.706	0.734	0.749	0.760	0.772	0.781	0.789	0.802	0.816	0.829
0.839	0.850	0.860	0.869	0.878	0.889	0.897	0.911	0.923	0.936	0.945	0.952	0.960
0.964	0.969	0.973	0.977	0.981	0.985	0.990	0.995	0.999				

Table 2 continued

	42.822			5.8662E-03		2.395						
0.313	0.580	0.675	0.713	0.741	0.757	0.766	0.775	0.783	0.789	0.799	0.802	0.809
0.817	0.823	0.829	0.839	0.848	0.858	0.869	0.883	0.904	0.919	0.931	0.947	0.960
0.969	0.981	0.988	0.993	0.999	0.999	0.999	0.999	0.999				
	44.339			5.7259E-03		2.375						
0.528	0.653	0.733	0.771	0.791	0.799	0.806	0.813	0.819	0.817	0.819	0.824	0.831
0.836	0.841	0.846	0.853	0.859	0.868	0.873	0.889	0.899	0.913	0.928	0.938	0.955
0.968	0.977	0.983	0.991	0.991	0.994	0.999	0.998	0.998				
	45.855			5.9894E-03		2.430						
0.426	0.623	0.666	0.694	0.719	0.731	0.745	0.757	0.765	0.773	0.787	0.798	0.804
0.811	0.819	0.822	0.828	0.837	0.845	0.854	0.870	0.893	0.912	0.930	0.951	0.969
0.979	0.989	0.993	0.998	0.997	0.999	0.999	0.998	0.998				
	47.370			5.8200E-03		2.460						
0.344	0.589	0.668	0.696	0.717	0.728	0.739	0.749	0.758	0.766	0.779	0.790	0.804
0.813	0.822	0.832	0.841	0.850	0.860	0.869	0.887	0.909	0.925	0.939	0.951	0.967
0.979	0.987	0.991	0.994	0.997	0.998	0.999	0.999	0.999				
	48.839			7.1678E-03		2.785						
0.430	0.569	0.621	0.653	0.677	0.699	0.709	0.723	0.735	0.743	0.759	0.772	0.782
0.791	0.799	0.805	0.813	0.821	0.827	0.835	0.851	0.869	0.885	0.901	0.918	0.939
0.955	0.969	0.979	0.988	0.989	0.993	0.995	0.997	0.999				
	50.342			7.2650E-03		2.500						
0.529	0.630	0.680	0.713	0.743	0.760	0.775	0.788	0.799	0.804	0.818	0.829	0.835
0.839	0.843	0.848	0.851	0.856	0.859	0.864	0.875	0.885	0.896	0.905	0.912	0.920
0.929	0.938	0.944	0.950	0.959	0.965	0.978	0.986	0.999				
	51.987			6.9186E-03		2.545						
0.539	0.620	0.660	0.687	0.708	0.721	0.735	0.746	0.753	0.762	0.773	0.784	0.795
0.803	0.813	0.823	0.833	0.840	0.848	0.855	0.871	0.884	0.897	0.909	0.923	0.938
0.951	0.962	0.971	0.977	0.982	0.989	0.992	0.999	0.999				
	53.739			5.7226E-03		2.525						
0.315	0.598	0.654	0.686	0.711	0.727	0.743	0.757	0.770	0.781	0.799	0.812	0.826
0.839	0.849	0.861	0.869	0.879	0.889	0.898	0.910	0.922	0.935	0.944	0.956	0.963
0.971	0.973	0.978	0.981	0.983	0.985	0.990	0.993	0.995				
	55.702			6.1270E-03		2.595						
0.569	0.671	0.705	0.726	0.743	0.759	0.764	0.773	0.782	0.791	0.805	0.813	0.817
0.829	0.835	0.843	0.851	0.861	0.868	0.875	0.894	0.909	0.922	0.934	0.944	0.951
0.959	0.969	0.973	0.980	0.983	0.986	0.989	0.993	0.997				

Table 2 continued

```
-1.54795E-06   2.48270E-04   -2.37901E-04
35
     3.648      9.9791E-04      2.400
0.300 0.660 0.819 0.862 0.899 0.917 0.933 0.945 0.959 0.967 0.978 0.987 0.991
0.994 0.994 0.997 0.995 0.999 0.998 0.997 0.997 0.999 0.999 0.999 0.999 0.999
0.999 0.999 0.999 0.999 0.999 0.999 0.999 0.999 0.999
     5.688      1.0803E-03      2.428
0.271 0.498 0.637 0.749 0.834 0.898 0.929 0.947 0.964 0.977 0.997 0.996 0.999
0.998 0.999 0.997 0.999 0.999 0.997 0.997 0.999 0.998 0.999 0.996 0.997 0.999
0.997 0.997 0.999 0.998 0.999 0.998 0.999 0.998 0.999
     7.125      1.1175E-03      2.439
0.175 0.348 0.515 0.677 0.773 0.850 0.918 0.941 0.963 0.979 0.999 0.999 0.999
0.999 0.999 0.999 0.999 0.999 0.999 0.999 0.997 0.998 0.999 0.999 0.998 0.999
0.999 0.999 0.999 0.999 0.999 0.999 0.999 0.999 0.998
     8.625      1.7856E-03      2.443
0.448 0.571 0.647 0.707 0.747 0.795 0.821 0.855 0.853 0.901 0.934 0.959 0.974
0.985 0.990 0.995 0.997 0.996 0.997 0.999 0.999 0.999 0.999 0.999 0.999 0.999
0.999 0.999 0.999 0.999 0.999 0.999 0.999 0.999 0.999
    10.094      2.0412E-03      2.453
0.319 0.474 0.598 0.675 0.731 0.775 0.807 0.834 0.854 0.871 0.905 0.931 0.951
0.967 0.977 0.985 0.989 0.997 0.998 0.999 0.999 0.999 0.999 0.999 0.999 0.999
0.999 0.999 0.999 0.999 0.999 0.999 0.999 0.999 0.999
    11.563      2.4657E-03      2.464
0.365 0.510 0.609 0.680 0.716 0.753 0.784 0.804 0.824 0.847 0.878 0.909 0.934
0.951 0.962 0.971 0.980 0.984 0.987 0.989 0.991 0.991 0.997 0.997 0.997 0.999
0.999 0.999 0.999 0.999 0.999 0.999 0.999 0.999 0.999
    13.094      4.5936E-03      2.482
0.389 0.544 0.616 0.661 0.696 0.723 0.746 0.766 0.782 0.799 0.822 0.843 0.861
0.879 0.890 0.902 0.911 0.920 0.927 0.931 0.941 0.950 0.955 0.960 0.967 0.973
0.979 0.981 0.987 0.991 0.995 0.998 0.999 0.999 0.999
    14.563      4.4877E-03      2.496
0.364 0.499 0.580 0.630 0.671 0.707 0.731 0.757 0.777 0.797 0.825 0.849 0.871
0.889 0.901 0.916 0.925 0.935 0.940 0.945 0.954 0.958 0.965 0.968 0.971 0.977
0.980 0.984 0.984 0.985 0.987 0.987 0.991 0.994 0.997
```

TABLE 3

DATA FOR CONCENTRATION 50 wppm

	16.063		3.5359E-03			2.515						
0.444	0.544	0.597	0.637	0.666	0.697	0.719	0.746	0.764	0.784	0.817	0.848	0.874
0.897	0.911	0.927	0.935	0.947	0.955	0.965	0.977	0.981	0.987	0.989	0.994	0.994
0.997	0.997	0.999	0.999	0.999	0.999	0.999	0.999	0.999				
	17.548		3.4059E-03			2.485						
0.396	0.582	0.659	0.705	0.737	0.765	0.790	0.803	0.819	0.832	0.853	0.870	0.887
0.901	0.913	0.920	0.929	0.936	0.942	0.949	0.960	0.969	0.979	0.989	0.993	0.997
0.999	0.999	0.999	0.999	0.999	0.999	0.999	0.999	0.999				
	19.000		3.7848E-03			2.540						
0.280	0.464	0.582	0.655	0.700	0.734	0.761	0.784	0.802	0.816	0.840	0.860	0.875
[illegible]	0.900	0.912	0.920	0.929	0.935	0.942	0.957	0.959	0.977	0.983	0.989	0.991
0.994	0.996	[illegible]	0.998	0.999	0.999	0.999	0.999	0.999				
	20.563		[illegible]			2.546						
0.191	0.374	0.557	0.636	0.675	[illegible]	0.727	0.747	0.766	0.780	0.804	0.819	0.836
0.851	0.867	0.881	0.894	0.906	0.917	[illegible]	[illegible]	0.958	0.971	0.977	0.985	0.991
0.994	0.995	0.997	0.997	0.997	0.998	0.999	0.999	[illegible]				
	22.031		4.2279E-03			2.553						
0.337	0.484	0.569	0.625	0.658	0.685	0.707	0.727	0.744	0.758	0.785	[illegible]	0.821
0.840	0.861	0.879	0.904	0.921	0.937	0.949	0.969	0.977	0.984	0.984	0.987	0.989
0.994	0.996	0.997	0.997	0.997	0.998	0.999	0.999	0.999				
	23.563		4.7206E-03			2.555						
0.267	0.437	0.565	0.619	0.661	0.691	0.711	0.730	0.747	0.759	0.780	0.799	0.815
0.829	0.847	0.864	0.880	0.900	0.915	0.929	0.949	0.961	0.969	0.977	0.979	0.984
0.985	0.986	0.990	0.994	0.999	0.999	0.999	0.999	0.999				
	25.063		5.1713E-03			2.560						
0.324	0.449	0.534	0.591	0.629	0.659	0.687	0.714	0.734	0.750	0.775	0.799	0.814
0.825	0.837	0.849	0.864	0.879	0.891	0.907	0.931	0.951	0.961	0.977	0.981	0.984
0.985	0.987	0.987	0.989	0.990	0.994	0.995	0.999	0.999				
	26.563		5.7073E-03			2.564						
0.329	0.464	0.547	0.597	0.629	0.657	0.684	0.700	0.715	0.728	0.751	0.770	0.787
0.805	0.817	0.829	0.841	0.857	0.869	0.885	0.909	0.928	0.945	0.959	0.969	0.977
0.984	0.984	0.989	0.994	0.994	0.997	0.999	0.999	0.999				
	28.265		5.5888E-03			3.045						
0.372	0.527	0.610	0.658	0.680	0.694	0.706	0.717	0.728	0.735	0.752	0.766	0.784
0.799	0.817	0.831	0.848	0.861	0.876	0.889	0.913	0.931	0.948	0.960	0.965	0.975
0.981	0.987	0.990	0.994	0.998	0.999	0.998	0.999	0.999				

Table 3 continued

	29.818		5.7385E-03			3.155						
0.384	0.551	0.615	0.652	0.667	0.686	0.699	0.709	0.715	0.720	0.734	0.745	0.762
0.776	0.796	0.807	0.825	0.841	0.859	0.871	0.898	0.921	0.940	0.955	0.969	0.983
0.990	0.999	0.999	0.999	0.999	0.999	0.999	0.999	0.999				
	31.000		6.0752E-03			2.575						
0.359	0.471	0.547	0.593	0.629	0.657	0.685	0.704	0.719	0.736	0.764	0.789	0.805
0.820	0.834	0.844	0.851	0.861	0.869	0.877	0.888	0.905	0.919	0.938	0.955	0.971
0.981	0.987	0.987	0.989	0.991	0.991	0.991	0.994	0.995				
	32.500		5.4204E-03			2.579						
0.247	0.419	0.507	0.569	0.607	0.637	0.671	0.695	0.715	0.731	0.761	0.785	0.804
0.820	0.830	0.838	0.859	0.869	0.879	0.896	0.919	0.941	0.961	0.970	0.976	0.980
0.985	0.989	0.990	0.991	0.992	0.993	0.994	0.995	0.996				
	34.000		6.1435E-03			2.585						
0.287	0.447	0.529	0.587	0.628	0.659	0.687	0.705	0.721	0.737	0.764	0.789	0.805
0.819	0.831	0.841	0.851	0.864	0.871	0.885	0.897	0.910	0.924	0.938	0.951	0.961
0.971	0.977	0.986	0.987	0.987	0.989	0.991	0.995	0.999				
	35.563		6.6369E-03			2.588						
0.380	0.507	0.557	0.605	0.634	0.657	0.677	0.696	0.711	0.725	0.749	0.769	0.785
0.804	0.817	0.829	0.841	0.856	0.866	0.877	0.895	0.909	0.927	0.937	0.944	0.954
0.964	0.967	0.971	0.977	0.980	0.984	0.985	0.989	0.999				
	37.094		7.3609E-03			2.593						
0.194	0.376	0.499	0.574	0.605	0.639	0.665	0.685	0.703	0.717	0.741	0.760	0.779
0.795	0.809	0.821	0.835	0.846	0.859	0.869	0.894	0.898	0.901	0.910	0.919	0.928
0.938	0.948	0.958	0.968	0.974	0.980	0.984	0.987	0.990				
	38.500		6.8029E-03			2.595						
0.377	0.500	0.559	0.597	0.625	0.647	0.667	0.685	0.699	.709	0.735	0.755	0.774
0.788	0.801	0.814	0.827	0.838	0.849	0.809	0.887	0.905	0.917	[illegible]	0.949	0.959
0.969	0.976	0.980	0.986	0.985	0.987	0.987	0.989	0.999				
	40.063		8.0734E-03			2.598						
0.361	0.497	0.543	0.584	0.612	0.630	0.651	0.665	0.679	0.690	0.711	0.734	0.747
0.764	0.776	0.790	0.801	0.809	0.824	0.834	0.854	0.876	0.884	0.897	0.911	0.924
0.934	0.945	0.955	0.964	0.973	0.982	0.989	0.992	0.998				
	41.500		7.3038E-03			2.600						
0.225	0.419	0.509	0.571	0.611	0.639	0.664	0.682	0.698	0.710	0.732	0.745	0.755
0.763	0.772	0.780	0.790	0.804	0.817	0.830	0.859	0.884	0.908	0.919	0.937	0.949
0.960	0.968	0.977	0.981	0.985	0.985	0.987	0.990	0.997				

Table 3 continued

	42.875		7.4394E-03			2.602						
0.339	0.487	0.554	0.597	0.629	0.654	0.677	0.694	0.707	0.719	0.741	0.759	0.771
0.787	0.799	0.807	0.819	0.827	0.839	0.847	0.865	0.887	0.910	0.927	0.937	0.945
0.955	0.959	0.964	0.967	0.969	0.970	0.977	0.981	0.994				
	44.563		8.1256E-03			2.603						
0.351	0.467	0.530	0.569	0.601	0.620	0.644	0.657	0.675	0.687	0.709	0.731	0.744
0.761	0.775	0.789	0.800	0.809	0.820	0.831	0.855	0.871	0.889	0.905	0.919	0.931
0.944	0.955	0.957	0.964	0.969	0.974	0.979	0.985	0.990				
	46.125		8.1428E-03			2.604						
0.217	0.419	0.524	0.577	0.614	0.639	0.661	0.679	0.697	0.709	0.731	0.751	0.767
0.785	0.799	0.809	0.821	0.831	0.841	0.854	0.869	0.884	0.895	0.905	0.915	0.925
0.934	0.939	0.947	0.957	0.967	0.975	0.981	0.986	0.990				
	47.563		7.9129E-03			2.605						
0.229	0.407	0.507	0.575	0.607	0.634	0.655	0.672	0.685	0.699	0.721	0.739	0.755
0.769	0.784	0.797	0.807	0.816	0.827	0.837	0.854	0.871	0.887	0.899	0.914	0.929
0.940	0.951	0.959	0.969	0.975	0.977	0.984	0.988	0.991				
	49.000		8.5119E-03			2.606						
0.368	0.484	0.538	0.571	0.595	0.617	0.635	0.652	0.669	0.682	0.709	0.733	0.751
0.768	0.779	0.792	0.802	0.810	0.819	0.828	0.842	0.858	0.872	0.887	0.899	0.916
0.929	0.940	0.949	0.960	0.967	0.974	0.979	0.984	0.990				
	50.500		8.0651E-03			2.606						
0.190	0.352	0.499	0.569	0.615	0.645	0.667	0.691	0.707	0.719	0.747	0.769	0.784
0.799	0.805	0.815	0.825	0.831	0.836	0.845	0.856	0.868	0.884	0.895	0.907	0.917
0.931	0.941	0.948	0.959	0.966	0.975	0.981	0.985	0.990				
	52.000		8.6167E-03			2.607						
0.306	0.455	0.525	0.573	0.600	0.629	0.646	0.665	0.684	0.695	0.719	0.737	0.754
0.767	0.774	0.784	0.791	0.799	0.806	0.814	0.827	0.844	0.859	0.880	0.897	0.915
0.934	0.947	0.957	0.964	0.969	0.974	0.979	0.985	0.990				
	54.063		8.4866E-03			2.607						
0.259	0.444	0.529	0.577	0.605	0.631	0.647	0.664	0.675	0.685	0.701	0.721	0.736
0.750	0.761	0.774	0.791	0.800	0.816	0.831	0.865	0.888	0.901	0.916	0.925	0.928
0.937	0.941	0.947	0.951	0.955	0.958	0.959	0.961	0.966				
	55.938		6.4122E-03			2.608						
0.467	0.574	0.627	0.667	0.685	0.705	0.722	0.735	0.747	0.759	0.779	0.799	0.811
0.827	0.837	0.851	0.865	0.875	0.886	0.891	0.907	0.917	0.929	0.934	0.939	0.947
0.954	0.961	0.967	0.977	0.976	0.981	0.985	0.985	0.986				

Table 3 continued

NØ.	X (IN)	THETA (FT)	THETAC	CF	U* (FT/S)	U1	RE
1	3.34	0.00038	0.00070	0.003882	0.097853	2.22	6.4432E 04
2	4.24	0.00073	0.00085	0.003852	0.096765	2.21	6.1214E 04
3	5.44	0.00073	0.00104	0.003811	0.096952	2.22	1.0488E 05
4	6.48	0.00210	0.00120	0.003776	0.096504	2.22	1.2483E 05
5	7.70	0.00178	0.00139	0.003734	0.100248	2.32	1.5509E 05
6	9.18	0.00220	0.00162	0.003684	0.095066	2.22	1.7651E 05
7	10.47	0.00235	0.00182	0.003640	0.094757	2.22	2.0178E 05
8	12.05	0.00207	0.00206	0.003587	0.094054	2.22	2.3236E 05
9	13.57	0.00254	0.00228	0.003535	0.093378	2.22	2.6153E 05
10	15.11	0.00230	0.00251	0.003483	0.092684	2.22	2.9127E 05
11	16.56	0.00479	0.00271	0.003434	0.092028	2.22	3.1919E 05
12	18.05	0.00310	0.00293	0.003383	0.093569	2.28	3.5638E 05
13	19.61	0.00360	0.00314	0.003330	0.107931	2.65	4.5020E 05
14	20.99	0.00328	0.00334	0.003283	0.108583	2.68	4.8843E 05
15	22.40	0.00371	0.00353	0.003235	0.110607	2.75	5.3472E 05
16	23.95	0.00367	0.00373	0.003183	0.106711	2.68	5.5618E 05
17	25.55	0.00427	0.00394	0.003128	0.105599	2.67	5.9224E 05
18	27.95	0.00360	0.00425	0.003047	0.095434	2.44	5.9321E 05
19	29.07	0.00423	0.00439	0.003009	0.090573	2.34	5.8912E 05
20	30.35	0.00413	0.00455	0.002966	0.093574	2.43	6.4015E 05
21	31.84	0.00455	0.00475	0.002912	0.090237	2.37	6.5573E 05
22	33.45	0.00489	0.00493	0.002860	0.089437	2.37	6.8681E 05
23	35.01	0.00554	0.00511	0.002807	0.090104	2.41	7.3100E 05
24	38.00	0.00583	0.00546	0.002706	0.089015	2.42	7.9826E 05
25	39.53	0.00503	0.00563	0.002654	0.086516	2.38	8.1500E 05
26	41.07	0.00471	0.00580	0.002602	0.089810	2.49	8.8767E 05
27	42.55	0.00552	0.00596	0.002551	0.089294	2.50	9.2346E 05
28	44.11	0.00617	0.00612	0.002499	0.098441	2.78	1.0663E 06
29	45.61	0.00685	0.00627	0.002448	0.096731	2.76	1.0947E 06
30	47.13	0.00667	0.00643	0.002396	0.092420	2.67	1.0922E 06
31	48.64	0.00701	0.00658	0.002345	0.092109	2.69	1.1357E 06
32	50.61	0.00647	0.00677	0.002278	0.090785	2.69	1.1818E 06
33	52.74	0.00732	0.00697	0.002206	0.089336	2.69	1.2314E 06
34	54.54	0.00665	0.00713	0.002145	0.088580	2.71	1.2806E 06
35	55.72	0.00471	0.00723	0.002105	0.085152	2.63	1.2697E 06

DRAG = 0.8158E-01 LBF

TABLE 4

CALCULATED PARAMETERS FOR CONCENTRATION 0 wppm

NØ.	X (IN)	THETA (FT)	THETAC	CF	U* (FT/S)	U1	RE
1	3.38	0.00106	0.00087	0.003674	0.108858	2.54	7.4502E 04
2	4.86	0.00112	0.00109	0.003630	0.111839	2.63	1.1072E 05
3	6.35	0.00110	0.00132	0.003587	0.101003	2.38	1.3155E 05
4	7.81	0.00113	0.00153	0.003544	0.103350	2.46	1.6646E 05
5	9.35	0.00173	0.00176	0.003500	0.102693	2.46	1.9934E 05
6	10.79	0.00208	0.00197	0.003458	0.103948	2.50	2.3422E 05
7	12.32	0.00228	0.00219	0.003413	0.097493	2.36	2.5241E 05
8	13.88	0.00261	0.00241	0.003368	0.096637	2.35	2.8374E 05
9	15.40	0.00266	0.00262	0.003323	0.093757	2.30	3.0751E 05
10	17.02	0.00269	0.00284	0.003276	0.094507	2.34	3.4498E 05
11	18.53	0.00313	0.00305	0.003232	0.105530	2.63	4.2219E 05
12	20.02	0.00312	0.00325	0.003189	0.102021	2.56	4.4411E 05
13	21.54	0.00333	0.00345	0.003145	0.103099	2.60	4.8606E 05
14	23.13	0.00331	0.00365	0.003099	0.103321	2.63	5.2694E 05
15	24.55	0.00388	0.00384	0.003057	0.102626	2.63	5.5945E 05
16	26.08	0.00426	0.00403	0.003012	0.098190	2.53	5.7274E 05
17	27.60	0.00454	0.00422	0.002968	0.097466	2.53	6.0610E 05
18	29.12	0.00452	0.00441	0.002924	0.100940	2.64	6.6742E 05
19	30.63	0.00499	0.00459	0.002880	0.098662	2.60	6.9130E 05
20	32.17	0.00438	0.00477	0.002835	0.097515	2.59	7.2322E 05
21	33.66	0.00543	0.00495	0.002792	0.096950	2.59	7.5832E 05
22	35.14	0.00481	0.00512	0.002749	0.088047	2.38	7.2437E 05
23	36.66	0.00447	0.00529	0.002704	0.087515	2.38	7.5747E 05
24	38.23	0.00466	0.00547	0.002659	0.084586	2.32	7.6995E 05
25	39.73	0.00583	0.00563	0.002615	0.085698	2.37	8.1732E 05
26	41.26	0.00575	0.00580	0.002570	0.085502	2.38	8.5419E 05
27	42.82	0.00587	0.00596	0.002525	0.085097	2.40	8.9027E 05
28	44.34	0.00573	0.00612	0.002481	0.083645	2.38	9.1411E 05
29	45.86	0.00599	0.00627	0.002437	0.084817	2.43	9.6725E 05
30	47.37	0.00582	0.00643	0.002392	0.085083	2.46	1.0115E 06
31	48.84	0.00717	0.00657	0.002350	0.095458	2.78	1.1807E 06
32	50.34	0.00727	0.00672	0.002306	0.084888	2.50	1.0925E 06
33	51.99	0.00692	0.00687	0.002258	0.085513	2.54	1.1485E 06
34	53.74	0.00572	0.00704	0.002207	0.083877	2.53	1.1779E 06
35	55.70	0.00613	0.00722	0.002150	0.085079	2.59	1.2547E 06

DRAG = 0.8222E-01 LBF

TABLE 5

CALCULATED PARAMETERS FOR CONCENTRATION 25 wppm

NØ.	X (IN)	THETA (FT)	THETAC	CF	U* (FT/S)	U1	RE
1	3.65	0.00100	0.00065	0.005687	0.127984	2.40	7.6000E 04
2	5.69	0.00108	0.00112	0.005536	0.127740	2.43	1.1988E 05
3	7.13	0.00112	0.00145	0.005429	0.127075	2.44	1.5085E 05
4	8.63	0.00179	0.00179	0.005318	0.125970	2.44	1.8291E 05
5	10.09	0.00204	0.00211	0.005208	0.125181	2.45	2.1494E 05
6	11.56	0.00247	0.00243	0.005099	0.124418	2.46	2.4732E 05
7	13.09	0.00459	0.00275	0.004986	0.123921	2.48	2.8211E 05
8	14.56	0.00449	0.00305	0.004876	0.123248	2.50	3.1553E 05
9	16.06	0.00354	0.00335	0.004765	0.122759	2.51	3.5068E 05
10	17.55	0.00341	0.00364	0.004655	0.119882	2.49	3.7853E 05
11	19.00	0.00378	0.00392	0.004547	0.121107	2.54	4.1892E 05
12	20.56	0.00434	0.00421	0.004431	0.119833	2.55	4.5446E 05
13	22.03	0.00423	0.00448	0.004322	0.118674	2.55	4.8824E 05
14	23.56	0.00472	0.00475	0.004208	0.117192	2.56	5.2260E 05
15	25.06	0.00517	0.00501	0.004096	0.115856	2.56	5.5696E 05
16	26.56	0.00571	0.00526	0.003985	0.114448	2.56	5.9121E 05
17	28.27	0.00559	0.00554	0.003858	0.133744	3.04	7.4711E 05
18	29.82	0.00574	0.00579	0.003743	0.136487	3.16	8.1663E 05
19	31.00	0.00608	0.00597	0.003655	0.110081	2.57	6.9293E 05
20	32.50	0.00542	0.00620	0.003544	0.108559	2.58	7.2758E 05
21	34.00	0.00614	0.00641	0.003432	0.107086	2.59	7.6293E 05
22	35.56	0.00664	0.00663	0.003316	0.105381	2.59	7.9893E 05
23	37.09	0.00736	0.00684	0.003202	0.103758	2.59	8.3494E 05
24	38.50	0.00680	0.00703	0.003098	0.102130	2.59	8.6725E 05
25	40.06	0.00807	0.00722	0.002982	0.100314	2.60	9.0350E 05
26	41.50	0.00730	0.00740	0.002875	0.098577	2.60	9.3663E 05
27	42.88	0.00744	0.00756	0.002773	0.096884	2.60	9.6841E 05
28	44.56	0.00813	0.00775	0.002647	0.094704	2.60	1.0069E 06
29	46.13	0.00814	0.00792	0.002531	0.092640	2.60	1.0426E 06
30	47.56	0.00791	0.00807	0.002424	0.090699	2.60	1.0755E 06
31	49.00	0.00851	0.00821	0.002318	0.088713	2.61	1.1085E 06
32	50.50	0.00807	0.00835	0.002206	0.086554	2.61	1.1424E 06
33	52.00	0.00862	0.00849	0.002095	0.084372	2.61	1.1768E 06
34	54.06	0.00849	0.00866	0.001942	0.081226	2.61	1.2235E 06
35	55.94	0.00641	0.00881	0.001802	0.078288	2.61	1.2664E 06

DRAG = 0.1135E 00 LBF

TABLE 6

CALCULATED PARAMETERS FOR CONCENTRATION 50 wppm